A REDUCED BASIS METHOD FOR COERCIVE EQUATIONS WITH AN EXACT SOLUTION CERTIFICATE AND SPATIO-PARAMETER ADAPTIVITY: ENERGY-NORM AND OUTPUT ERROR BOUNDS

MASAYUKI YANO*

Abstract. We develop a reduced basis method for linear coercive parametrized partial differential equations (PDEs) with two objectives: providing an energy-norm or functional-output *a posteriori* error bound with respect to the exact weak solution of the PDE as opposed to the typical finite element "truth" solution; providing reliable and efficient construction of a reduced basis model through automatic adaptivity in both physical and parameter spaces. Our error bounds build on two key ingredients. The first is a minimum-residual mixed formulation which provides an approximate solution as well as an upper bound of the dual norm of the residual with respect to the infinite-dimensional function space. The second is an extension of the successive constraint method (SCM) to evaluate a lower bound of the stability constant with respect to the infinite-dimesional function space; the approach builds on a computable lower bound of the minimum eigenvalue associated with the stability constant. Both the minimum-residual mixed formulation and the extended SCM admit offline-online computational decomposition. The offline stage incorporates spatial mesh adaptation and greedy parameter sampling for both the solution approximation and the stability eigenproblem to yield a reliable online system in an efficient manner. The online stage provides an approximate solution and an *a posteriori* error bound with respect to the exact solution for any parameter value in complexity independent of the size of the finite element spaces. We demonstrate the effectiveness of the approach for a thermal block problem, which exhibits parameter-dependent spatial singularities.

Key words. reduced basis method, *a posteriori* error bounds, minimum-residual mixed method, offline-online decomposition, successive constraint method, spatio-parameter adaptivity

AMS subject classifications. 65N15, 65N30, 65N35

1. Introduction.

The goal of the certified reduced basis method is to provide rapid and reliable predictions of functional outputs associated with parametrized partial differential equations (PDEs) in real-time and many-query applications [18]. The rapidness is provided by an offline-online computational decomposition; the reliability is provided by *a posteriori* error bounds. The classical certified reduced basis method provides *a posteriori* error bounds with respect to the finite element "truth" solution computed in a finite-dimensional "truth" space, which is *assumed* to be sufficiently rich such that the difference between the "truth" solution and the exact weak solution of the PDE is negligible. In practice, this assumption is not rigorously verified and may be violated for problems that exhibit complex parameter-dependent spatial features. An under-refined mesh results in inaccurate predictions and unreliable error bounds with respect to the exact solution. Conversely, an over-refined mesh results in unnecessarily expensive finite element snapshot solves in the offline stage. A typical "truth" mesh suffers from both of these problems as the mesh is under-refined in some regions and over-refined in other regions. The goal of this work is to eliminate the issue of "truth" within the classical reduced basis framework; we will develop a reduced basis method that provides online-efficient *a posteriori* error bounds with respect to the exact weak solution in the energy norm as well as for linear functional outputs.

The present work builds on, and addresses the major limitation of, our previous work [23]. The major limitation of [23] is that the error is assessed in a dual-norm of the residual, which, while equivalent to the energy norm, quantitatively does not hold any engineering significance. The true value of model reduction in engineering contexts is only realized if the method provides predictions and associated error bounds for quantities of interest, expressed in terms of output functionals. The ingredients required to provide error bounds for quantities of interest using an adjoint-based formulation are the same as those associated with the energy-norm of the error. Hence in this work we focus on providing online-offline computable error bounds both in the energy norm and for functional outputs.

Our energy-norm and functional-output error bounds build on two key ingredients: an upper bound of the dual norm of the residual and a lower bound of the stability constant. Our method provides, in the online stage, uniform (as opposed to asymptotic) bounds for the dual norm of the residual and the stability constant, both of which are with respect to the infinite-dimesional function space as opposed to the typical finite element "truth" space. We adhere to the standard reduced basis goals with regard to the offline-

*Institute for Aerospace Studies, University of Toronto, Toronto, ON, Canada (myano@utias.utoronto.ca).

online computational efficiency and online certification: i) the online solution is computed in complexity independent of the underlying finite element discretization; ii) the online error bound is provided for any parameter value and not just those in the training set. Providing an error bound with respect to the exact solution is a recent idea in the reduced basis community; we here note related work by Ali *et al.* [2], Ohlberger and Schindler [12], and ourselves [22, 23].

Our approximation of the solution field is based on a version of the minimum-residual mixed reduced basis method [23], which belongs to a family of least-squares methods (see, e.g., [3, 14]). The mixed formulation simultaneously computes both the (primal) solution and a dual solution, the latter of which provides a bound for the dual norm of the (primal) residual. The use of the dual solution to provide an error bound is similar to the complementary variational principle, which has been extensively applied to finite element methods by, for example, Ladevèze and Leguillion [11], Ainsworth and Oden [1], and Sauer-Budge *et al.* [19] and more recently to a reduced basis method [22]. However, our approach [23] differs from the classical complementary variational principle in that it does not require a space that exactly satisfies dual-feasibility conditions, construction of which in an offline-online efficient manner can be done in some limited cases [22] but to our knowledge cannot be accomplished in general. This "relaxation" is accomplished by considering a dual norm of the residual with respect to a norm that is different from the energy norm. However, as a consequence of not using the energy norm, the stability constant is not unity and we must compute a lower bound of the stability constant to bound the error; in this work we extend our minimum-residual mixed formulation [23] to incorporate a carefully chosen, parameter-dependent norm which facilitate the construction of error bounds in the energy norm or for functional outputs.

Providing a lower bound of the stability constant requires the evaluation of a lower bound of the minimum eigenvalue associated with an eigenproblem. It is well-known that an upper bound of the minimum eigenvalue can be readily computed by any Galerkin method, but a lower bound is much more complicated to compute; for brevity, we will not attempt to provide a comprehensive overview of eigenvalue bounds and instead refer to a review paper by Plum [15]. Our formulation is based on the method by Weinstein (see [4], Chapter 6), which provides a lower bound using the eigenproblem residual or "defect" under the assumption that the minimum eigenvalue associated with the finite element approximation is closer to the minimum eigenvalue of the exact problem than to the second smallest eigenvalue. In the offline stage, we provide a bound for the eigenproblem residual using a mixed formulation similar to that for the solution residual. We then appeal to the successive constraint method (SCM) of Huynh *et al.* [7], which to our knowledge is the only method that can provide a uniform (as opposed to asymptotic) lower bound of the stability constant in an offline-online efficient manner. Specifically, we extend the original SCM — which was designed to provide a stability constant with respect to a "truth" finite element space — to provide lower bounds of stability constants with respect to the infinite-dimesional function space. Our formulation also incorporates a transformation of the original stability constant such that the effectivity of the stability constant is desensitized from the relatively poor effectivity of the SCM lower bound.

The contributions of this work are fivefold. First, we develop a minimum-residual mixed formulation whose dual variable provides a built-in bound of a dual norm of the residual with respect to a parametrized norm. Second, we extend the SCM to evaluate a lower bound of the stability constant with respect to an infinite-dimensional function space; here, we appeal to Weinstein's method to express a lower bound of the minimum eigenvalue in terms of the eigenproblem residual and then develop a mixed formulation to bound the dual norm of the residual. Third, we develop a transformation of the stability constant such that the bound gap for the stability constant is desensitized from the SCM bound gap. Fourth, we develop spatio-parameter adaptation strategies based on isotropic-h mesh adaptation and greedy parameter sampling for both the stability eigenproblem and the solution approximation. Fifth, we demonstrate the effectiveness of the spatio-parameter adaptive strategy for the classical thermal block problem [18], which is defined in a high-dimensional parameter space and exhibits parameter-dependent spatial singularities.

Before we conclude the introduction, we note the limitations of the error bounds developed in this work. The first limitation is related to the evaluation of the lower bound of the stability constant. As noted, one of the ingredients of our error bounds is a lower bound of the stability constant, which is equivalent to a lower bound of the minimum eigenvalue associated with a parametrized eigenproblem. We appeal to Weinstein's method to construct a lower bound. As a consequence, in the offline approximation of the minimum eigenvalue, we assume that the minimum eigenvalue associated with the Galerkin finite element

approximation of the eigenproblem is closer to the minimum eigenvalue than the second smallest eigenvalue of the exact eigenproblem. We unfortunately do not have any means to verify if this assumption is satisfied. However, in practice for many elliptic equations, the eigenfunction associated with the minimum eigenvalue is the easiest to approximate, and hence this assumption is often satisfied even on a very coarse mesh.

The second limitation is the class of equations to which the error bound formulation applies; namely, the formulation applies only to coercive equations. To our knowledge, this is a limitation shared by all error bound techniques that provide uniform (as opposed to asymptotic) error bounds (as opposed to estimates); see, e.g., [19, 13, 9, 10]. Coercivity, or the convexity property, is the key to the construction of uniform error bounds in these works, and our present work is no exception. However, we note that the two important classes of problems in mechanics — heat transfer and elasticity — are coercive, and the efficacy of uniform error bounds and adaptivity for numerical approximation of heat-transfer and elasticity problems have been demonstrated in the aforementioned works.

This paper is organized as follows. Section 2 introduces the problem considered throughout this paper, defines function spaces, and presents a well-known proposition that identifies key ingredients of our error bounds. Section 3 introduces a minimum-residual mixed formulation and devise an associated offline-online computational strategy. Section 4 presents an extension of the SCM to infinite-dimensional function spaces, including the computation of a lower bound of the stability constant with respect to the exact space. Section 5 presents our error bounds. Section 6 presents two spatio-parameter adaptive strategies, one associated with the stability constant and the other associated with the solution field. Section 7 assesses the effectiveness of the proposed strategy using the classical thermal block problem. Finally, we summarize the work in Section 8.

2. Preliminaries.

2.1. Problem statement. We first introduce a d-dimensional bounded spatial domain $\Omega \subset \mathbb{R}^d$, for $d = 1, 2, 3$, with a Lipschitz boundary $\partial\Omega$; the boundary is decomposed into a Dirichlet boundary Γ_D, which is assumed non-empty, and a Neumann boundary Γ_N such that $\overline{\partial\Omega} = \overline{\Gamma}_D \cup \overline{\Gamma}_N$. We also introduce a P-dimensional bounded parameter domain $\mathcal{D} \subset \mathbb{R}^P$. We then introduce a Sobolev space

$$\mathcal{V} \equiv \{v \in H^1(\Omega) \mid v|_{\Gamma_D} = 0\},$$

where $H^1(\Omega)$ is the standard H^1 Sobolev space (see, e.g., [16]). We now consider the following weak statement: given $\mu \in \mathcal{D}$, find $u(\mu) \in \mathcal{V}$ such that

$$a(u(\mu), v; \mu) = \ell(v; \mu) \quad \forall v \in \mathcal{V}, \tag{1}$$

where

$$a(w, v; \mu) \equiv \int_\Omega \nabla v \cdot K(\mu) \nabla w dx \quad \forall w, v \in \mathcal{V},$$
$$\ell(v; \mu) \equiv \int_\Omega v f(\mu) dx + \int_{\Gamma_N} v g(\mu) ds \quad \forall v \in \mathcal{V}.$$

Here, $K : \mathcal{D} \to [L^\infty(\Omega)]^{d\times d}$ is a symmetric diffusivity field, $f : \mathcal{D} \to L^2(\Omega)$ is a source function, and $g : \mathcal{D} \to L^2(\Gamma_N)$ is a Neumann boundary data; note that each function is parametrized.

We make a few assumptions about the forms that define the problem. First, we assume that $K(\mu)$ is uniformly positive in the sense that the minimum eigenvalue of $K(\mu)(x)$ is bounded from below: $\lambda_{\min}(K(\mu)(x)) \geq K_{\min} > 0$ almost everywhere in Ω for all $\mu \in \mathcal{D}$. Second, we assume that $K(\mu)$, $f(\mu)$, and $g(\mu)$ admit decompositions that are affine in functions of the parameter:

$$K(\mu) = \sum_{q=1}^{Q_K} \Theta_q^K(\mu) K_q, \quad f(\mu) = \sum_{q=1}^{Q_f} \Theta_q^f(\mu) f_q, \quad g(\mu) = \sum_{q=1}^{Q_g} \Theta_q^g(\mu) g_q,$$

where $K_q \in (L^\infty(\Omega))^{d\times d}$, $f_q \in L^2(\Omega)$, and $g_q \in L^2(\Gamma_N)$ are parameter-independent fields, and $\Theta_q^K \in L^\infty(\mathcal{D})$, $\Theta_q^f \in L^\infty(\mathcal{D})$, and $\Theta_q^g \in L^\infty(\mathcal{D})$ are parameter-dependent functions. Third, we assume that $K^{-1}(\mu)$ admits

a decomposition that is affine in functions of parameter:

$$K^{-1}(\mu) = \sum_{q=1}^{Q_{K^{\text{inv}}}} \Theta_q^{K^{\text{inv}}}(\mu) K_q^{\text{inv}}, \tag{2}$$

where $K_q^{\text{inv}} \in (L^\infty(\Omega))^{d\times d}$ is a parameter-independent field, and $\Theta_q^{K^{\text{inv}}} \in L^\infty(\mathcal{D})$ is a parameter-dependent function; note that K_q^{inv} is in general not related to K_q. (This assumption can be relaxed; see Remark 1.) Finally, we assume that fields K_q, f_q, g_q, and K_q^{inv} are piecewise polynomials such that we can evaluate integrals involving the fields exactly using quadrature rules.

In this work, we develop a reduced basis method that approximates the solution to (1) and provides an associated error bound. Specifically, we provide a sequence of approximations $u_N(\mu)$, $N = 1, 2, \ldots$, to $u(\mu)$ and associated error bounds $\Delta_N(\mu)$, $N = 1, 2, \ldots$, such that

$$|||u(\mu) - u_N(\mu)|||_\mu \leq \Delta_N(\mu), \quad N = 1, 2, \ldots,$$

where $|||\cdot|||_\mu$ is the energy norm given by $|||w|||_\mu \equiv \sqrt{a(w, w; \mu)}$. In addition, given a bounded linear functional $\ell^o(\cdot; \mu)$ that admits an affine parameter decomposition and the associated true output $s(\mu) \equiv \ell^o(u(\mu); \mu)$, we provide a sequence of approximate outputs $s_N(\mu)$, $N = 1, 2, \ldots$, and associated error bounds $\Delta_N^s(\mu)$, $N = 1, 2, \ldots$, such that

$$|s(\mu) - s_N(\mu)| \leq \Delta_N^s(\mu), \quad N = 1, 2, \ldots;$$

we note that the output bound is of interest in engineering practice.

REMARK 1. *We make a few remarks regarding the assumption (2). First, we may develop an alternative formulation — which also provides an error bound with respect to the exact solution — that does not rely on this assumption; the construction of this alternative bound is discussed in Appendix A. Second, the assumption (2) allows us to construct an error bound with a higher effectivity by permitting a more flexible choice of the norm with respect to which the dual norm of the residual and the stability constant are computed. Third, many problems of practical interest admit an affine decomposition of $K^{-1}(\mu)$, including those problems involving piecewise-affine geometry transformations that are often used in reduced basis formulations (see, e.g., [18]). For instance, the methodology for parametrized linear elasticity problems with geometry transformations is demonstrated in [24].*

REMARK 2. *In this work we consider scalar equations to simplify the presentation. However, our approximation and error bound procedures readily extend to vector-valued equations. (See, e.g., [24].)*

2.2. Inner products and norms. We introduce two different inner products that simplify the presentation of the proposed method. First is the parametrized inner product

$$(w, v)_{\mathcal{V}(\mu;\delta)} \equiv \int_\Omega \nabla v \cdot K(\mu) \nabla w dx + \delta \int_\Omega vw dx + \delta \int_{\Gamma_N} vw ds \quad \forall w, v \in \mathcal{V}$$

and the associated induced norm $\|w\|_{\mathcal{V}(\mu;\delta)} \equiv \sqrt{(w, w)_{\mathcal{V}(\mu;\delta)}}$ for a parameter $\mu \in \mathcal{D}$ and a weight $\delta \in \mathbb{R}_{>0}$. Note that this parametrized norm is related to the energy norm by $\|w\|^2_{\mathcal{V}(\mu;\delta)} = |||w|||^2_\mu + \delta\|w\|^2_{L^2(\Omega)} + \delta\|w\|^2_{L^2(\Gamma_N)}$. In addition, by the Poincaré-Friedrichs inequality and the trace theorem, the norm $\|\cdot\|_{\mathcal{V}(\mu;\delta)}$ is equivalent to the energy norm $|||\cdot|||_\mu$, which in turn is equivalent to $\|\cdot\|_{H^1(\Omega)}$ for all $\mu \in \mathcal{D}$.

Second is the parametrized inner product

$$(p, q)_{\mathcal{K}(\mu)} \equiv \int_\Omega q \cdot K(\mu) p dx \quad \forall p, q \in (L^2(\Omega))^d$$

and the associated induced norm $\|p\|_{\mathcal{K}(\mu)} \equiv \sqrt{(p, p)_{\mathcal{K}(\mu)}}$. Note that the energy norm may be expressed as $|||w|||_\mu = \|\nabla w\|_{\mathcal{K}(\mu)}$. Because the field $K(\mu)$ is bounded and positive, the norm $\|\cdot\|_{\mathcal{K}(\mu)}$ is equivalent to $\|\cdot\|_{L^2(\Omega)}$ for all $\mu \in \mathcal{D}$.

2.3. Energy-norm error bound. We now introduce the two ingredients that constitutes our error bound: the dual-norm of the residual and the stability constant. We first introduce the residual functional: for $\mu \in \mathcal{D}$ and $\tilde{u} \in \mathcal{V}$,

$$r(v;\tilde{u};\mu) \equiv \ell(v;\mu) - a(\tilde{u},v;\mu) \quad \forall v \in \mathcal{V};$$

the dual norm of the residual is given by

$$\|r(\cdot;\tilde{u};\mu)\|_{\mathcal{V}'(\mu;\delta)} \equiv \sup_{v\in\mathcal{V}} \frac{r(v;\tilde{u};\mu)}{\|v\|_{\mathcal{V}(\mu;\delta)}}. \tag{3}$$

We then introduce a stability constant

$$\alpha(\mu;\delta) \equiv \inf_{v\in\mathcal{V}} \frac{|||v|||_\mu^2}{\|v\|_{\mathcal{V}(\mu;\delta)}^2}. \tag{4}$$

The following well-known proposition provides an energy-norm error bound. (See, e.g., [16]).

PROPOSITION 3. *For any $\mu \in \mathcal{D}$ and $\tilde{u} \in \mathcal{V}$, the energy norm of the error is bounded by*

$$|||u(\mu) - \tilde{u}|||_\mu \le \frac{1}{(\alpha(\mu;\delta))^{1/2}} \|r(\cdot;\tilde{u};\mu)\|_{\mathcal{V}'(\mu;\delta)}.$$

Proof. For $e \equiv u(\mu) - \tilde{u}$, we obtain

$$\begin{aligned} |||e|||_\mu &= \frac{a(e,e;\mu)}{|||e|||_\mu} = \frac{r(e;\tilde{u};\mu)}{|||e|||_\mu} = \frac{\|e\|_{\mathcal{V}(\mu;\delta)}}{|||e|||_\mu} \frac{r(e;\tilde{u};\mu)}{\|e\|_{\mathcal{V}(\mu;\delta)}} \le \sup_{v\in\mathcal{V}} \frac{\|v\|_{\mathcal{V}(\mu;\delta)}}{|||v|||_\mu} \sup_{v\in\mathcal{V}} \frac{r(v;\tilde{u};\mu)}{\|v\|_{\mathcal{V}(\mu;\delta)}} \\ &= \left(\inf_{v\in\mathcal{V}} \frac{|||v|||_\mu}{\|v\|_{\mathcal{V}(\mu;\delta)}} \right)^{-1} \sup_{v\in\mathcal{V}} \frac{r(v;\tilde{u};\mu)}{\|v\|_{\mathcal{V}(\mu;\delta)}} = \frac{1}{(\alpha(\mu;\delta))^{1/2}} \|r(\cdot;\tilde{u};\mu)\|_{\mathcal{V}'(\mu;\delta)}; \end{aligned}$$

here, the first equality follows from the definition of the energy norm $|||\cdot|||_\mu$, the second equality follows from the error-residual relationship, and the last equality follows from the definitions of the stability constant and the dual-norm of the residual. ∎

The proposition shows that the evaluation of an upper bound of the energy-norm of the error requires an upper bound of the dual norm of the residual and a lower bound of the stability constant.

2.4. Error bound for linear functional outputs. Our energy-norm error bound may be extended to provide an error bound for a linear functional output $s(\mu) = \ell^o(u(\mu);\mu)$ where

$$\ell^o(w,\mu) \equiv \int_\Omega w f^o(\mu) dx + \int_{\Gamma_N} w g^o(\mu) ds \quad \forall w \in \mathcal{V}. \tag{5}$$

Here, $f^o : \mathcal{D} \to L^2(\Omega)$ is the volume output function, and $g^o : \mathcal{D} \to L^2(\Gamma_N)$ is the boundary output function; we assume f^o and g^o admit decompositions that are affine in functions of parameters. Our error-bound approach follows that for the standard reduced basis method [18] and appeals to the following well-known proposition regarding the output error. (See, e.g., Giles and Süli [6], Section 4.)

PROPOSITION 4. *We define the adjoint problem: given $\mu \in \mathcal{D}$, find $\psi(\mu) \in \mathcal{V}$ such that*

$$a(v,\psi(\mu);\mu) = \ell^o(v;\mu) \quad \forall v \in \mathcal{V}. \tag{6}$$

For a primal approximation $\tilde{u} \in \mathcal{V}$ and an adjoint approximation $\tilde{\psi} \in \mathcal{V}$, we introduce an adjoint-corrected output

$$\tilde{s}(\mu) \equiv \ell^o(\tilde{u};\mu) + r(\tilde{\psi};\tilde{u};\mu).$$

Then, the error in the output prediction is bounded by

$$|s(\mu) - \tilde{s}(\mu)| \leq \frac{1}{\alpha(\mu;\delta)} \|r(\cdot;\tilde{u};\mu)\|_{\mathcal{V}'(\mu;\delta)} \|r_{\rm adj}(\cdot;\tilde{\psi};\mu)\|_{\mathcal{V}'(\mu;\delta)}, \tag{7}$$

where $\alpha(\mu;\delta)$ is the stability constant (4) and the adjoint residual $r_{\rm adj}(\cdot;\cdot;\cdot)$ is defined by

$$r_{\rm adj}(v;\tilde{\psi};\mu) \equiv \ell^o(v;\mu) - a(v,\tilde{\psi};\mu) \quad \forall v \in \mathcal{V}.$$

Proof. We note that

$$\begin{aligned}
|s(\mu) - \tilde{s}(\mu)| &= |\ell^o(u(\mu);\mu) - \ell^o(\tilde{u};\mu) - r(\tilde{\psi};\tilde{u};\mu)| = |\ell^o(u(\mu) - \tilde{u};\mu) - a(u(\mu) - \tilde{u},\tilde{\psi};\mu)| \\
&= |r_{\rm adj}(u(\mu) - \tilde{u};\tilde{\psi};\mu)| \leq \|r_{\rm adj}(\cdot;\tilde{\psi};\mu)\|_{\mathcal{V}'(\mu;\delta)} \|u(\mu) - \tilde{u}\|_{\mathcal{V}(\mu;\delta)} \\
&\leq \|r_{\rm adj}(\cdot;\tilde{\psi};\mu)\|_{\mathcal{V}'(\mu;\delta)} \frac{1}{(\alpha(\mu;\delta))^{1/2}} |||u(\mu) - \tilde{u}|||_\mu \leq \|r_{\rm adj}(\cdot;\tilde{\psi};\mu)\|_{\mathcal{V}'(\mu;\delta)} \frac{1}{\alpha(\mu;\delta)} \|r(\cdot;\tilde{u};\mu)\|_{\mathcal{V}'(\mu;\delta)}.
\end{aligned}$$

Here, the first, second, and third equality follows from the definitions of $\tilde{s}(\mu)$, $r(\cdot;\cdot;\cdot)$, and $r_{\rm adj}(\cdot;\cdot;\cdot)$, respectively; the first, second, and third inequality follows from the definition of the dual norm, the definition of $\alpha(\mu;\delta)$, and the bound on $|||u(\mu) - \tilde{u}|||_\mu$, respectively. ∎

The proposition shows that the evaluation of a bound for a functional output requires a lower bound of the stability constant, an upper bound of the dual norm of the (primal) residual, and an upper bound of the dual norm of the adjoint residual. As the same technique can be used to bound the dual norm of the primal and adjoint residuals, bounding the output error requires the same set of ingredients as bounding the energy norm of the error.

3. An offline-online computable upper bound of the dual norm of the residual.

3.1. Residual bound form. We now develop a computable upper bound of the dual-norm of the residual (3). The proposed residual bound procedure is a generalization of the procedure introduced in [23] to the parametrized norm $\|\cdot\|_{\mathcal{V}(\mu;\delta)}$.

We first introduce a vector-valued Hilbert space

$$Q \equiv H^1(\text{div};\Omega) \equiv \{q \in (L^2(\Omega))^d \mid \nabla \cdot q \in L^2(\Omega)\},$$

endowed with an inner product $(w,v)_{\mathcal{Q}} \equiv (w,v)_{H^1(\text{div};\Omega)} \equiv \int_\Omega (\nabla \cdot w)(\nabla \cdot v) dx + \int_\Omega w \cdot v dx$ and the induced norm $\|w\|_{\mathcal{Q}} \equiv \sqrt{(w,w)_{\mathcal{Q}}}$. The following proposition provides a bound of the dual norm of the residual.

PROPOSITION 5. *For any $\mu \in \mathcal{D}$, $\delta \in \mathbb{R}_{>0}$, and $\tilde{u} \in \mathcal{V}$, the dual norm of the residual is bounded by*

$$\|r(\cdot;\tilde{u};\mu)\|_{\mathcal{V}'(\mu;\delta)} \leq (F(\tilde{u},q;\mu;\delta))^{1/2} \quad \forall q \in \mathcal{Q},$$

where the bound form is given by

$$F(\tilde{u},q;\mu;\delta) = \|\nabla\tilde{u} - K^{-1}(\mu)q\|^2_{\mathcal{K}(\mu)} + \delta^{-1}\|f(\mu) + \nabla\cdot q\|^2_{L^2(\Omega)} + \delta^{-1}\|g(\mu) - q\cdot n\|^2_{L^2(\Gamma_N)}. \tag{8}$$

Proof. We note that for any $\tilde{u} \in \mathcal{V}$, $v \in \mathcal{V}$, and $q \in \mathcal{Q}$,

$$
\begin{aligned}
& r(v;\tilde{u};\mu) \\
& = \ell(v;\mu) - a(\tilde{u},v;\mu) \\
& = \int_\Omega v f(\mu) dx + \int_{\Gamma_N} v g(\mu) ds - \int_\Omega \nabla v \cdot K(\mu) \nabla \tilde{u} dx \\
& = \int_\Omega v f(\mu) dx + \int_{\Gamma_N} v g(\mu) ds - \int_\Omega \nabla v \cdot K(\mu) \nabla \tilde{u} dx + \int_\Omega \nabla v \cdot q dx + \int_\Omega v \nabla \cdot q dx - \int_{\Gamma_N} v q \cdot n ds \\
& = \int_\Omega v (f(\mu) + \nabla \cdot q) dx - \int_\Omega \nabla v \cdot (K(\mu)\nabla \tilde{u} - q) dx + \int_{\Gamma_N} v (g(\mu) - q \cdot n) ds \\
& \le \|v\|_{L^2(\Omega)} \|f(\mu) + \nabla \cdot q\|_{L^2(\Omega)} + \|\nabla v\|_{\mathcal{K}(\mu)} \|\nabla \tilde{u} - K^{-1}(\mu) q\|_{\mathcal{K}(\mu)} + \|v\|_{L^2(\Gamma_N)} \|g(\mu) - q \cdot n\|_{L^2(\Gamma_N)} \\
& \le (\delta \|v\|^2_{L^2(\Omega)} + \|\nabla v\|^2_{\mathcal{K}(\mu)} + \delta \|v\|^2_{L^2(\Gamma_N)})^{1/2} \\
& \qquad (\delta^{-1} \|f(\mu) + \nabla \cdot q\|^2_{L^2(\Omega)} + \|\nabla \tilde{u} - K^{-1}(\mu) q\|^2_{\mathcal{K}(\mu)} + \delta^{-1} \|g(\mu) - q \cdot n\|_{L^2(\Gamma_N)^2})^{1/2} \\
& = \|v\|_{\mathcal{V}(\mu;\delta)} (F(\tilde{u},q;\mu;\delta))^{1/2};
\end{aligned}
$$

here the third equality follows from the Green's theorem. It thus follows that

$$
\|r(v;\tilde{u};\mu)\|_{\mathcal{V}'(\mu;\delta)} \equiv \sup_{v \in \mathcal{V}} \frac{r(v;\tilde{u};\mu)}{\|v\|_{\mathcal{V}(\mu;\delta)}} \le (F(\tilde{u},q;\mu;\delta))^{1/2},
$$

which is the desired inequality. ∎

We make a few observations as regard the behavior of the primal bound form (8) with the weight δ. In the case of vanishing parameter $\delta = 0$, the bound form (8) evaluates to

$$
F(\tilde{u},q;\mu;\delta \equiv 0) = \begin{cases} \|\nabla \tilde{u} - K^{-1}(\mu) q\|^2_{\mathcal{K}(\mu)} & \forall \tilde{u} \in \mathcal{V},\ \forall q \in \mathcal{Q}^*(\mu), \\ \infty \quad \text{otherwise}, \end{cases}
$$

where the constrained space $\mathcal{Q}^*(\mu)$ is given by

$$
\mathcal{Q}^*(\mu) = \{ q \in \mathcal{Q} \mid f(\mu) + \nabla \cdot q = 0 \text{ in } L^2(\Omega)\ ;\ g(\mu) - q \cdot n = 0 \text{ in } L^2(\Gamma_N) \}. \tag{9}
$$

The condition (9) is precisely the dual-feasibility condition for the complementary variational principle. The exact satisfaction of the dual feasibility condition is possible in the finite-element context, as pursued by, for instance, Ladevèze and Leguillion [11], Ainsworth and Oden [1], and Sauer-Budge *et al.* [19]. On the other hand, the exact satisfaction of the dual feasibility condition in the reduced-basis context, as pursued in [22], requires a special construction of reduced-basis spaces with limited practicality. Hence, in the present context, we choose a small but non-zero δ to relax the dual-feasibility requirement; a practical rule for selecting a δ is discussed in Section 6.3.

3.2. Decomposition of the bound form. In order to facilitate the development of finite-element and reduced-basis approximations, we introduce a decomposition of the form $F(\cdot,\cdot;\mu;\delta)$ defined in (8) into quadratic, linear, and constant terms. The form (8) may be expressed as

$$
F(w,q;\mu;\delta) = G(\{w,q\},\{w,q\};\mu;\delta) - 2L(\{w,q\};\mu;\delta) + H(\mu;\delta), \tag{10}
$$

where the bilinear form, linear form, and constant term are given by

$$
G(\{w,p\},\{v,q\};\mu;\delta) \equiv G_0(\{w,p\},\{v,q\};\mu) + \delta^{-1} G_\Omega(p,q) + \delta^{-1} G_{\Gamma_N}(p,q), \tag{11}
$$

$$
\begin{aligned}
L(\{v,q\};\mu;\delta) &\equiv \delta^{-1} L_\Omega(q;\mu) + \delta^{-1} L_{\Gamma_N}(q;\mu), \\
H(\mu;\delta) &\equiv \delta^{-1} H_\Omega(\mu) + \delta^{-1} H_{\Gamma_N}(\mu),
\end{aligned} \tag{12}
$$

for

$$
\begin{aligned}
G_0(\{w,p\},\{v,q\};\mu) &\equiv \int_\Omega \left[q\cdot K^{-1}(\mu)p - q\cdot\nabla w - \nabla v\cdot p + \nabla v\cdot K(\mu)\nabla w\right] dx \\
&= \sum_{a=1}^{Q_{K^{\rm inv}}} \Theta_a^{K^{\rm inv}}(\mu)\int_\Omega q\cdot K_a^{\rm inv} p dx - \int_\Omega q\cdot\nabla w dx - \int_\Omega \nabla v\cdot p dx \\
&\quad + \sum_{a=1}^{Q_K}\Theta_a^K(\mu)\int_\Omega \nabla v\cdot K_a\nabla w dx, \\
G_\Omega(p,q) &\equiv \int_\Omega (\nabla\cdot q)(\nabla\cdot p)dx, \\
G_{\Gamma_N}(p,q) &\equiv \int_{\Gamma_N}(q\cdot n)(p\cdot n)ds, \\
L_\Omega(q;\mu) &\equiv \int_\Omega(-\nabla\cdot q)f(\mu)dx = \sum_{a=1}^{Q_f}\Theta_a^f(\mu)\int_\Omega(-\nabla\cdot q)f_a dx, \\
L_{\Gamma_N}(q;\mu) &\equiv \int_{\Gamma_N}(q\cdot n)g(\mu)ds = \sum_{a=1}^{Q_g}\Theta_a^g(\mu)\int_\Omega (q\cdot n)g_a ds, \\
H_\Omega(\mu) &\equiv \int_\Omega f(\mu)f(\mu)dx = \sum_{a,b=1}^{Q_f}\Theta_a^f(\mu)\Theta_b^f(\mu)\int_\Omega f_a f_b dx, \\
H_{\Gamma_N}(\mu) &\equiv \int_{\Gamma_N} g(\mu)g(\mu)ds = \sum_{a,b=1}^{Q_g}\Theta_a^g(\mu)\Theta_b^g(\mu)\int_\Omega g_a g_b ds.
\end{aligned}
$$

We note that the parametrized forms associated with the bound form $F(\cdot,\cdot;\mu;\delta)$ inherit the affine parameter decomposition of the fields $K(\mu)$, $K^{-1}(\mu)$, $f(\mu)$, and $g(\mu)$. As we will see in Section 3.5, and as in the standard reduced basis method [18], this affine parameter decomposition plays a key role in offline-online computational decomposition.

3.3. Minimum-bound mixed finite element method. We first introduce a sequence of conforming, non-degenerate triangulations $\mathcal{T}_h$ of Ω. We then introduce conforming finite-element approximation spaces for $\mathcal{V}$ and $\mathcal{Q}$:

$$
\mathcal{V}^{\mathcal{N}_\mathcal{V}} \equiv \{v\in\mathcal{V} \mid v|_\kappa \in \mathbb{P}^p,\ \forall \kappa\in\mathcal{T}_h\}, \tag{13}
$$

$$
\mathcal{Q}^{\mathcal{N}_\mathcal{Q}} \equiv \{q\in\mathcal{Q} \mid q|_\kappa \in \mathbb{RT}^{p-1} \equiv (\mathbb{P}^{p-1})^d \oplus x\mathbb{P}^{p-1},\ \forall \kappa\in\mathcal{T}_h\}; \tag{14}
$$

note that $\mathcal{V}^{\mathcal{N}_\mathcal{V}}$ consists of the standard H^1 conforming elements and $\mathcal{Q}^{\mathcal{N}_\mathcal{Q}}$ consists of Raviart-Thomas elements [17] of degree $p-1$ (see, e.g., [16], Chapter 7). The superscripts $\mathcal{N}_\mathcal{V}$ and $\mathcal{N}_\mathcal{Q}$ denote the number of degrees of freedom associated with the spaces $\mathcal{V}^{\mathcal{N}_\mathcal{V}}$ and $\mathcal{Q}^{\mathcal{N}_\mathcal{Q}}$, respectively. We in addition set $\mathcal{N}\equiv\mathcal{N}_\mathcal{V}+\mathcal{N}_\mathcal{Q}$, which serves as a measure of the complexity of the finite-element approximation.

We now consider the minimum-bound solution: given $\mu\in\mathcal{D}$ and $\delta\in\mathbb{R}_{>0}$, find $\{w^\mathcal{N}(\mu),p^\mathcal{N}(\mu)\}\in \mathcal{V}^{\mathcal{N}_\mathcal{V}}\times\mathcal{Q}^{\mathcal{N}_\mathcal{Q}}$ such that

$$
\{w^\mathcal{N}(\mu),p^\mathcal{N}(\mu)\} = \inf_{\substack{w\in\mathcal{V}^{\mathcal{N}_\mathcal{V}}\\ q\in\mathcal{Q}^{\mathcal{N}_\mathcal{Q}}}} F(w,q;\mu;\delta). \tag{15}
$$

We identify the associated Euler-Lagrange equation: given $\mu\in\mathcal{D}$ and $\delta\in\mathbb{R}_{>0}$, find $\{w^\mathcal{N}(\mu),p^\mathcal{N}(\mu)\}\in\mathcal{V}^{\mathcal{N}_\mathcal{V}}\times\mathcal{Q}^{\mathcal{N}_\mathcal{Q}}$ such that

$$
G(\{w^\mathcal{N}(\mu),p^\mathcal{N}(\mu)\},\{v,q\};\mu;\delta) = L(\{v,q\};\mu;\delta)\quad \forall\{v,q\}\in\mathcal{V}^{\mathcal{N}_\mathcal{V}}\times\mathcal{Q}^{\mathcal{N}_\mathcal{Q}},
$$

where G is the bilinear form (11) and L is the linear form (12). The problem is well posed thanks to the coercivity of the bilinear form $G(\cdot,\cdot;\mu;\delta)$ with respect to $\mathcal{V}\times\mathcal{Q}$ and the fact $\mathcal{V}^{\mathcal{N}_\mathcal{V}}\subset\mathcal{V}$ and $\mathcal{Q}^{\mathcal{N}_\mathcal{Q}}\subset\mathcal{Q}$. Once we obtain the finite element approximation, we readily bound the dual norm of the residual using $\|r(\cdot;u^{\mathcal{N}}(\mu);\mu)\|_{\mathcal{V}'(\mu;\delta)}\le(F(u^{\mathcal{N}}(\mu),p^{\mathcal{N}}(\mu);\mu;\delta))^{1/2}$.

3.4. Minimum-bound mixed reduced basis method. We consider our minimum-output-bound reduced basis approximation. Towards this end, we introduce an N-dimensional primal approximation space spanned by a basis $\{\xi_n\}_{n=1}^N$,

$$\mathcal{V}_N=\text{span}\{\xi_n\}_{n=1}^N\subset\mathcal{V}^{\mathcal{N}_\mathcal{V}},$$

and an N-dimensional dual approximation space spanned by a basis $\{\eta_n\}_{n=1}^N$,

$$\mathcal{Q}_N=\text{span}\{\eta_n\}_{n=1}^N\subset\mathcal{Q}^{\mathcal{N}_\mathcal{Q}}.$$

We then consider the minimum-bound solution: given $\mu\in\mathcal{D}$ and $\delta\in\mathbb{R}_{>0}$, find $\{u_N(\mu),p_N(\mu)\}\in\mathcal{V}_N\times\mathcal{Q}_N$ such that

$$\{u_N(\mu),p_N(\mu)\}=\arg\inf_{\substack{w\in\mathcal{V}_N\\ q\in\mathcal{Q}_N}}F(w,q;\mu;\delta). \tag{16}$$

We identify the associated Euler-Lagrange equation: given $\mu\in\mathcal{D}$ and $\delta\in\mathbb{R}_{>0}$, find $\{u_N(\mu),p_N(\mu)\}\in\mathcal{V}_N\times\mathcal{Q}_N$ such that

$$G(\{u_N(\mu),p_N(\mu)\},\{v,q\};\mu;\delta)=L(\{v,q\};\mu;\delta)\quad\forall\{v,q\}\in\mathcal{V}_N\times\mathcal{Q}_N, \tag{17}$$

where G is the bilinear form (11) and L is the linear form (12). The problem is again well posed thanks to the coercivity of the bilinear form $G(\cdot,\cdot;\mu;\delta)$ with respect to $\mathcal{V}\times\mathcal{Q}$ and the fact $\mathcal{V}_N\subset\mathcal{V}$ and $\mathcal{Q}_N\subset\mathcal{Q}$. Once we obtain the reduced basis approximation, we readily bound the dual norm of the residual using $\|r(\cdot;u_N(\mu);\mu)\|_{\mathcal{V}'(\mu;\delta)}\le(F(u_N(\mu),p_N(\mu);\mu;\delta))^{1/2}$.

REMARK 6. *Our formulation readily accommodates primal and dual reduced basis spaces of different dimensions. However, in practice, we use the spaces of the same dimension because these basis functions are associated with the finite element approximation at select parameter values:* $\mathcal{V}_N=span\{\xi_n\}_{n=1}^N=span\{u^{\mathcal{N}}(\mu^{(n)})\}_{n=1}^N$ *and* $\mathcal{Q}_N=span\{\eta_n\}_{n=1}^N=span\{p^{\mathcal{N}}(\mu^{(n)})\}_{n=1}^N$. *An adaptive procedure for selecting the snapshots will be described in Section 6.5.*

3.5. Offline-online computational decomposition. We now present an offline-online computational procedure for the reduced basis method. We here appeal to the decomposition of the primal bound (10) into bilinear forms, linear forms, and constant terms. Specifically, for $w\equiv\sum_{n=1}^N\xi_n\mathbf{w}_n\in\mathcal{V}_N$, $p\equiv\sum_{n'=1}^N\eta_{n'}\mathbf{p}_{n'}\in\mathcal{Q}_N$, $v\equiv\sum_{m=1}^N\xi_m\mathbf{v}_m\in\mathcal{V}_N$, and $q\equiv\sum_{m'=1}^N\eta_{m'}\mathbf{q}_{m'}\in\mathcal{Q}_N$ in the reduced basis spaces, the terms that

constitute (10) evaluate to

$$
\begin{aligned}
G_0(\{w,p\},\{v,q\};\mu) &= \mathbf{q}_{m'} \sum_{a=1}^{Q_{K^{\rm inv}}} \Theta_a^{K^{\rm inv}}(\mu) \left[\int_\Omega \eta_{m'} \cdot K_a^{\rm inv} \eta_{n'} dx\right] \mathbf{p}_{n'} - \mathbf{q}_{m'} \left[\int_\Omega \eta_{m'} \cdot \nabla \xi_n dx\right] \mathbf{w}_n \\
&\quad - \mathbf{v}_m \left[\int_\Omega \nabla \xi_m \cdot \eta_{n'} dx\right] \mathbf{p}_{n'} + \mathbf{v}_m \sum_{a=1}^{Q_K} \Theta_a^K(\mu) \left[\int_\Omega \nabla \xi_m \cdot K_a \nabla \xi_n dx\right] \mathbf{w}_n \\
G_\Omega(p,q) &= \mathbf{q}_{m'} \left[\int_\Omega \nabla \cdot \eta_{m'} \nabla \cdot \eta_{n'} dx\right] \mathbf{p}_{n'}, \\
G_{\Gamma_N}(p,q) &= \mathbf{q}_{m'} \left[\int_{\Gamma_N} (\eta_{m'} \cdot n)(\eta_{n'} \cdot n) ds\right] \mathbf{p}_{n'}, \\
L_\Omega(q;\mu) &= \mathbf{q}_{m'} \sum_{a=1}^{Q_f} \Theta_a^f(\mu) \left[\int_\Omega (-\nabla \cdot \eta_{m'}) f_a dx\right], \\
L_{\Gamma_N}(q;\mu) &= \mathbf{q}_{m'} \sum_{a=1}^{Q_g} \Theta_a^g(\mu) \left[\int_{\Gamma_N} (\eta_{m'} \cdot n) g_a dx\right], \\
H_\Omega(\mu) &= \sum_{a,b=1}^{Q_f} \Theta_a^f(\mu) \Theta_b^f(\mu) \left[\int_\Omega f_a f_b dx\right], \\
H_{\Gamma_N}(\mu) &= \sum_{a,b=1}^{Q_g} \Theta_a^g(\mu) \Theta_b^g(\mu) \left[\int_{\Gamma_N} g_a g_b dx\right];
\end{aligned}
$$

here the summation on the repeated m', n', m, and n are implied. In the offline stage, we compute the terms appearing in brackets, $[\cdot]$. In the online stage, we first assemble the matrices and vectors with appropriate weights $\Theta_\cdot^\cdot(\mu)$ evaluated for the parameter value of interest. We then solve the primal reduced basis system (17) of the size $2N$ to obtain the coefficients $\mathbf{u}_N(\mu) \in \mathbb{R}^N$ and $\mathbf{p}_N(\mu) \in \mathbb{R}^N$ of the primal solution. We finally appeal to the decomposition (10) to evaluate the bound of the dual-norm of the primal residual, $F(u_N(\mu), p_N(\mu); \mu; \delta)$.

4. An offline-online computable lower bound of the stability constant.

4.1. Transformation of the stability constant. We now consider a offline-online computable lower bound of the stability constant (4), $\alpha(\mu;\delta) \equiv \inf_{v\in\mathcal{V}} |||v|||_\mu^2 / \|v\|_{\mathcal{V}(\mu;\delta)}^2$. By way of preliminaries, we introduce an inner product

$$
(w,v)_{\mathcal{W}} \equiv (w,v)_{H^1(\Omega)} + (w,v)_{L^2(\Gamma_N)} \tag{18}
$$

and the associated induced norm $\|w\|_{\mathcal{W}} \equiv \sqrt{(w,w)_{\mathcal{W}}}$. We now present a proposition that relates the stability constant $\alpha(\mu;\delta)$ to another quantity $\tau(\mu)$, which is amenable to offline-online computational decomposition.

PROPOSITION 7. *The stability constant $\alpha(\mu;\delta) \equiv \inf_{v\in\mathcal{V}} |||v|||_\mu^2 / \|v\|_{\mathcal{V}(\mu;\delta)}^2$ is bounded from the below by*

$$
\alpha(\mu;\delta) \geq \left(1 + \frac{\delta}{\tau_{\rm LB}(\mu)}\right)^{-1}
$$

where $\tau_{\rm LB}(\mu)$ satisfies

$$
\tau_{\rm LB}(\mu) \leq \tau(\mu) \equiv \inf_{v\in\mathcal{V}} \frac{|||v|||_\mu^2}{\|v\|_{\mathcal{W}}^2}. \tag{19}
$$

Proof. We note that

$$\frac{1}{\alpha(\mu;\delta)} \equiv \left(\inf_{v\in\mathcal{V}} \frac{|||v|||_\mu^2}{\|v\|_{\mathcal{V}(\mu;\delta)}^2}\right)^{-1} = \sup_{v\in\mathcal{V}} \frac{\|v\|_{\mathcal{V}(\mu;\delta)}^2}{|||v|||_\mu^2} = \sup_{v\in\mathcal{V}} \frac{|||v|||_\mu^2 + \delta\|v\|_{L_2(\Omega)}^2 + \delta\|v\|_{L^2(\Gamma_N)}^2}{|||v|||_\mu^2}$$
$$= \sup_{v\in\mathcal{V}} \left(1 + \delta\frac{\|v\|_{L_2(\Omega)}^2 + \|v\|_{L^2(\Gamma_N)}^2}{|||v|||_\mu^2}\right) \le 1 + \delta \sup_{v\in\mathcal{V}} \frac{\|v\|_{\mathcal{W}}^2}{|||v|||_\mu^2} = 1 + \frac{\delta}{\tau(\mu)};$$

here, the first equality follows from the definition of the stability constant, the third equality follows from the definition of $|||\cdot|||_\mu$ and $\|v\|_{\mathcal{V}(\mu;\delta)}$, the inequality follows from $\|v\|_{L^2(\Omega)}^2 + \|v\|_{L^2(\Gamma_N)}^2 \le \|v\|_{\mathcal{W}}^2$, and the last equality follows from the definition of $\tau(\mu)$. We obtain the desired result by noting that $\tau_{\rm LB}(\mu) \le \tau(\mu)$. ∎

We make four observations. First, the proposition shows that if we can compute a lower bound of $\tau(\mu)$ in an offline-online efficient manner, then we can rapidly evaluate a lower bound of $\alpha(\mu;\delta)$. Second, we observe that the lower bound of $\alpha(\mu;\delta)$ is close to unity if δ is chosen small with respect to $\tau_{\rm LB}(\mu)$; more specifically, the transformation allows us to desensitize the effectivity of a lower bound of $\alpha(\mu;\delta)$ from the effectivity of a lower bound of $\tau(\mu)$ by choosing $\delta \ll \tau_{\rm LB}(\mu)$. Third, we observe that for $\delta \equiv 0$ the stability constant is unity; we recall that the minimum-bound solution for $\delta \equiv 0$ must satisfy the dual-feasibility condition (9) exactly, and for such a solution by complementary variational principle, the dual norm of the residual is the same as the energy-norm of the error, which implies the stability constant is unity. Fourth, we observe that $\tau(\mu) \equiv |||v|||_\mu^2/\|v\|_{\mathcal{W}}^2$ admits an affine parameter decomposition, as $|||\cdot|||_\mu^2 \equiv a(\cdot,\cdot;\mu)$ admits an affine decomposition and the norm $\|\cdot\|_{\mathcal{W}}^2$ is independent of the parameter; this property of $\tau(\mu)$ makes it suitable for offline-online computation by the successive constraint method.

Using an argument based on the Rayleigh quotient, we can readily show the quantity $\tau(\mu)$ is the minimum eigenvalue of the following eigenproblem: given $\mu \in \mathcal{D}$, find $(z_i(\mu), \lambda_i(\mu)) \in \mathcal{V} \times \mathbb{R}$ such that $\|z_i(\mu)\|_{\mathcal{W}} = 1$ and

$$a(z_i(\mu), v; \mu) = \lambda_i(\mu)(z_i(\mu), v)_{\mathcal{W}} \quad \forall v \in \mathcal{V} \tag{20}$$

for indices $i = 1, 2, \ldots$. We will henceforth refer to this eigenproblem as the stability eigenproblem. Without loss of generality, we order the eigenvalues in ascending order; hence $\tau(\mu) = \lambda_1(\mu)$, where the subscript 1 denotes the first eigenvalue. Hence, to provide a lower bound of $\tau(\mu)$, we need to provide a lower bound of $\lambda_1(\mu)$.

4.2. Successive constraint method (SCM). Our approach to compute a lower bound of $\tau(\mu)$ in an offline-online efficient manner is based on the successive constraint method (SCM) of Huynh *et al.* [7]. The original SCM was introduced to compute a lower bound of the stability constant with respect to *the finite-dimensional finite element space*; here we extend the method to provide a lower bound of the stability constant with respect to *the infinite-dimensional space* $\mathcal{V}$. We here present only a brief overview of the SCM and refer to [7] for a more detailed presentation; we will however highlight the key differences between the original SCM and our extension.

The SCM, as the name suggests, recasts the minimization problem associated with $\tau(\mu)$ as a linear constrained optimization problem. Towards this end, we first introduces the space

$$\mathcal{Y} \equiv \left\{ y \in \mathbb{R}^{Q_K} \mid \exists v_y \in \mathcal{V} \text{ s.t. } y_q = \frac{\int_\Omega \nabla v_y \cdot K_q \nabla v_y dx}{\|w_y\|_{\mathcal{W}}^2},\ q = 1, \ldots, Q_K \right\}$$

and the functional

$$\mathcal{J}(\mu; y) \equiv \sum_{q=1}^{Q_K} \Theta_q^K(\mu) y_q.$$

We then note that the quantity $\tau(\mu)$ can be expressed as

$$\tau(\mu) = \inf_{y\in\mathcal{Y}} \mathcal{J}(\mu; y).$$

To evaluate a lower bound of the stability constant, we now introduce a space $\mathcal{Y}_{\rm LB} \supset \mathcal{Y}$ given by

$$\mathcal{Y}_{\rm LB}(\Xi_{\rm con}) \equiv \left\{ y \in B_{Q_K} \mid \sum_{q=1}^{Q_K} \Theta_q^K(\mu') y_q \geq \tau(\mu'),\ \forall \mu' \in \Xi_{\rm con} \right\}; \tag{21}$$

here B_{Q_K} is a bounding box defined by

$$B_{Q_K} \equiv \prod_{q=1}^{Q_K} [\gamma_q^-, \gamma_q^+]$$

for

$$\gamma_q^- \equiv \inf_{v \in \mathcal{V}} \frac{\int_\Omega \nabla v \cdot K_q \nabla v dx}{\|v\|_{\mathcal{W}}^2}, \quad q = 1, \ldots, Q_K, \tag{22}$$

$$\gamma_q^+ \equiv \sup_{v \in \mathcal{V}} \frac{\int_\Omega \nabla v \cdot K_q \nabla v dx}{\|v\|_{\mathcal{W}}^2}, \quad q = 1, \ldots, Q_K, \tag{23}$$

and $\Xi_{\rm con} \subset \mathcal{D}$ is a set of "SCM constrained points" that are chosen in a careful manner (e.g., using a greedy algorithm). We then define a lower bound of the stability constant as

$$\tau_{\rm LB}(\mu) = \inf_{y \in \mathcal{Y}_{\rm LB}(\Xi_{\rm con})} \mathcal{J}(\mu; y);$$

here, $\tau_{\rm LB}(\mu) \leq \tau(\mu)$ because $\mathcal{Y}_{\rm LB} \supset \mathcal{Y}$.

We note that $\tau_{\rm LB}(\mu)$ admits offline-online computational decomposition: in the offline stage, we compute the set $\{\tau(\mu')\}_{\mu' \in \Xi_{\rm con}}$, and the set $\{\gamma_q^\pm\}_{q=1}^{Q_K}$, which together define the space $\mathcal{Y}_{\rm LB}(\Xi_{\rm con})$; in the online stage, we solve the linear programming problem $\tau_{\rm LB}(\mu) = \inf_{y \in \mathcal{Y}_{\rm LB}(\Xi_{\rm con})} \mathcal{J}(\mu; y)$ to find a lower bound for a given μ.

The two key differences between the original SCM [7] and our extension for $\tau(\mu)$ with respect to the infinite-dimesional space $\mathcal{V}$ are the following. First, the constants $\gamma_q^\pm$, $q = 1, \ldots, Q_K$, defined in (22) and (23) require infimization and supremization over $\mathcal{V}$, as opposed to a finite element space $\mathcal{V}^\mathcal{N}$ for the original SCM. Second, the constraints $\tau(\mu')$ defined in (19) require infimization over $\mathcal{V}$, as opposed to $\mathcal{V}^\mathcal{N}$. Because these supremization and infimization problems are defined over an infinite-dimesional space $\mathcal{V}$, they cannot be computed directly. We now present our strategies to provide computable bounds for these quantities.

4.3. Offline evaluation of an upper bound of $\gamma_q^\pm$. To evaluate γ_q^+, we appeal to

$$\gamma_q^+ \equiv \sup_{v \in \mathcal{V}} \frac{\int_\Omega \nabla v \cdot K_q \nabla v dx}{\|v\|_{\mathcal{W}}^2} \leq \sup_{v \in \mathcal{V}} \frac{\int_\Omega \nabla v \cdot K_q \nabla v dx}{|v|_{H^1(\Omega)}^2} \leq \|\lambda_{\max}(K_q(x))\|_{L^\infty(\Omega)} \equiv \tilde{\gamma}_q^+. \tag{24}$$

Because the fields $K_q \in [L^\infty(\Omega)]^{d \times d}$ are known, we can directly compute the upper bounds. Similarly, to evaluate γ_q^-, we appeal to

$$\gamma_q^- \equiv \inf_{v \in \mathcal{V}} \frac{\int_\Omega \nabla v \cdot K_q \nabla v dx}{\|v\|_{\mathcal{W}}^2} \geq -\sup_{v \in \mathcal{V}} \frac{|\int_\Omega \nabla v \cdot K_q \nabla v dx|}{\|v\|_{\mathcal{W}}^2} \geq -\|\lambda_{\max}(K_q(x))\|_{L^\infty(\Omega)} \equiv \tilde{\gamma}_q^-. \tag{25}$$

While the above expression for $\tilde{\gamma}_q^-$ works in general, K_q sometimes possess a special structure such that a tighter bound for γ_q^- can be obtained; for instance, if K_q is positive, then γ_q^- is bounded from below by 0.

4.4. An abstract lower bound of the minimum eigenvalue. In order to express a lower bound of the minimum eigenvalue using Weinstein's method, we define a residual associated with the eigenproblem (20): for $\mu \in \mathcal{D}$, $\tilde{z} \in \mathcal{V}$ with $\|\tilde{z}\|_{\mathcal{W}} = 1$, and $\tilde{\lambda} \in \mathbb{R}$,

$$r_{\rm eig}(v; \tilde{z}, \tilde{\lambda}; \mu) \equiv a(\tilde{z}, v; \mu) - \tilde{\lambda}(\tilde{z}, v)_{\mathcal{W}} \quad \forall v \in \mathcal{V}. \tag{26}$$

The associated dual norm of the eigenproblem residual with respect to $\|\cdot\|_{\mathcal{W}}$ is

$$\|r_{\text{eig}}(\cdot;\tilde{z},\tilde{\lambda};\mu)\|_{\mathcal{W}'} \equiv \sup_{v\in\mathcal{V}} \frac{r_{\text{eig}}(\cdot;\tilde{z},\tilde{\lambda};\mu)}{\|v\|_{\mathcal{W}}}.$$

The following proposition by Weinstein relates the dual norm of the residual — which is called the *defect* in the original work — to the distance to the closest eigenvalue.

PROPOSITION 8 (Weinstein's method [4], Chapter 6). *Let $(\tilde{z},\tilde{\lambda}) \in \mathcal{V}\times\mathbb{R}$ be an approximate eigenpair where $\|\tilde{z}\|_{\mathcal{W}} = 1$. Then, the distance between $\tilde{\lambda}$ and the closest eigenvalue is bounded from the above by*

$$\min_{j=1,2,\ldots} |\lambda_j(\mu) - \tilde{\lambda}| \le \|r_{\text{eig}}(\cdot;\tilde{z},\tilde{\lambda};\mu)\|_{\mathcal{W}'}.$$

Proof. For notational convenience, throughout this proof, we suppress the dependence of the bilinear form $a(\cdot,\cdot;\mu)$, the residual form $r_{\text{eig}}(\cdot;\cdot,\cdot;\mu)$, and the eigenvalues $\{z_i(\mu)\}$ on the parameter $\mu\in\mathcal{D}$. We denote the coefficients associated with the representation of an arbitrary vector $v\in\mathcal{V}$ in the eigenbasis $\{z_i\}_{i=1}^{\infty}$ by $\hat{v}$ such that $v = \sum_{n=1}^{\infty}\hat{v}_n z_n$. Similarly, we denote the coefficients associated with the representation of the approximate eigenvector $\tilde{z}$ in the eigenbasis by $\hat{\tilde{z}}$ such that $\tilde{z} = \sum_{n=1}^{\infty}\hat{\tilde{z}}_n z_n$. The inequality then follows from

$$\begin{aligned}
\|r_{\text{eig}}(\cdot;\tilde{z},\tilde{\lambda})\|_{\mathcal{W}'} &= \sup_{v\in\mathcal{V}} \frac{a(\tilde{z},v) - \tilde{\lambda}(\tilde{z},v)_{\mathcal{W}}}{\|v\|_{\mathcal{W}}} = \sup_{\substack{\hat{v}\\ \sum_{n=1}^{\infty}\hat{v}_n z_n\in\mathcal{V}}} \frac{\sum_{m,n=1}^{\infty}\hat{v}_m\hat{\tilde{z}}_n[a(z_n,z_m) - \tilde{\lambda}(z_n,z_m)_{\mathcal{W}}]}{(\sum_{m,n=1}^{\infty}\hat{v}_m\hat{v}_n(z_n,z_m)_{\mathcal{W}})^{1/2}} \\
&= \sup_{\substack{\hat{v}\\ \sum_{n=1}^{\infty}\hat{v}_n z_n\in\mathcal{V}}} \frac{\sum_{n}^{\infty}\hat{v}_n\hat{\tilde{z}}_n(\lambda_n-\tilde{\lambda})}{(\sum_{n=1}^{\infty}\hat{v}_n^2)^{1/2}} = (\sum_{n=1}^{\infty}\hat{\tilde{z}}_n^2(\lambda_n-\tilde{\lambda})^2)^{1/2} \\
&\ge \min_{n=1,2,\ldots}|\lambda_n-\tilde{\lambda}|(\sum_{n=1}^{\infty}\hat{\tilde{z}}_n^2)^{1/2} = \min_{n=1,2,\ldots}|\lambda_n-\tilde{\lambda}|\|\tilde{z}\|_{\mathcal{W}} = \min_{n=1,2,\ldots}|\lambda_n-\tilde{\lambda}|.
\end{aligned}$$

A few explanations are in order. The third equality follows from the definition of the eigenvalues and the orthogonality of the eigenbasis with respect to $a(\cdot,\cdot)$ and $(\cdot,\cdot)_{\mathcal{W}}$: $a(z_n,z_m) = \lambda_n$ if $n=m$ and $a(z_n,z_m)=0$ if $n\neq m$; $(z_n,z_m)_{\mathcal{W}} = 1$ if $n=m$ and $(z_n,z_m)_{\mathcal{W}}=0$ if $n\neq m$. The fourth equality follows from the fact that the supremizer is $\hat{v}_n = \hat{\tilde{z}}_n(\lambda_n-\tilde{\lambda})$, $n=1,2,\ldots$. The last equality follows from $\|\tilde{z}\|_{\mathcal{W}}=1$. ∎

We appeal to the proposition to provide a lower bound of the minimum eigenvalue under one crucial assumption:

COROLLARY 9. *Let $(\tilde{z},\tilde{\lambda})\in\mathcal{V}\times\mathbb{R}$ be an approximate eigenpair where $\|\tilde{z}\|_{\mathcal{W}}=1$. If $|\lambda_1(\mu)-\tilde{\lambda}| \le |\lambda_2(\mu)-\tilde{\lambda}|$ then*

$$\lambda_1(\mu) \ge \tilde{\lambda} - \|r_{\text{eig}}(\cdot;\tilde{z},\tilde{\lambda};\mu)\|_{\mathcal{W}'}.$$

We make two remarks. First, we unfortunately have no means to rigorously verify whether the condition $|\lambda_1(\mu)-\tilde{\lambda}| \le |\lambda_2(\mu)-\tilde{\lambda}|$ is satisfied; this, as noted in the Introduction, is a crucial limitation as regard the rigorousness of error bounds provided by our method. However, we have found that in practice the first two eigenvalues of (20) are sufficiently well separated for a typical elliptic problem that even a crude finite element approximation of the eigenproblem is sufficient to meet the condition. Hence, if we could compute an upper bound of the dual norm of the eigenproblem residual, then we can provide a lower bound of $\lambda_1(\mu) = \tau(\mu)$.

Second, the bound based on Weinstein's method is not very effective. Specifically, there exists another bound technique by Kato [8] which provides a lower bound whose gap scales as the square of the residual instead of linearly with the residual [15]. However, Kato's method introduces an additional assumption regarding the *second* eigenvalue of the eigenproblem. Here, we sacrifice the effectivity for the robustness of making one fewer assumptions and build our algorithm on Weinstein's method. We also note that thanks to the desensitization provided by the transformation of $\alpha(\mu;\delta)$ to $\tau(\mu)$, the loss of effectivity in a lower bound of $\tau(\mu)$ does not significantly affect the effectivity of the resulting lower bound of $\alpha(\mu;\delta)$.

4.5. Eigenproblem residual bound form. In order to construct a computable lower bound of $\lambda_1(\mu)$, we now develop a computable upper bound of the dual norm of the eigenproblem residual (26). Our approach is similar to the bounding technique developed in Section 3.1 to bound the dual norm of the (solution) residual. The following proposition provides a bound of the dual norm of the eigenproblem residual.

PROPOSITION 10. *For any $\mu \in \mathcal{D}$, $\tilde{z} \in \mathcal{V}$ such that $\|\tilde{z}\|_{\mathcal{W}} = 1$, and $\tilde{\lambda} \in \mathbb{R}$, the dual norm of the eigenproblem residual is bounded by*

$$\|r_{\text{eig}}(\cdot; \tilde{z}, \tilde{\lambda}; \mu)\|_{\mathcal{W}'} \le (F_{\text{eig}}(\tilde{z}, \tilde{\lambda}, q; \mu))^{1/2} \quad \forall q \in \mathcal{Q},$$

where the bound form is given by

$$F_{\text{eig}}(\tilde{z}, \tilde{\lambda}, q; \mu) = \tilde{\lambda}^2(\|\nabla \cdot q + \tilde{z}\|^2_{L^2(\Omega)} + \|q - \tilde{\lambda}^{-1}K(\mu)\nabla\tilde{z} + \nabla\tilde{z}\|^2_{L^2(\Omega)} + \|q \cdot n - \tilde{z}\|^2_{L^2(\Gamma_N)}). \tag{27}$$

Proof. We note that, for all $\tilde{z} \in \mathcal{V}$, $v \in \mathcal{V}$, $\tilde{\lambda} \in \mathbb{R}$, and $q \in \mathcal{Q}$,

$$\begin{aligned}
r_{\text{eig}}(v; \tilde{z}, \tilde{\lambda}; \mu) &= \int_\Omega \nabla v \cdot K(\mu)\nabla\tilde{z}dx - \tilde{\lambda}\int_\Omega (\nabla v \cdot \nabla\tilde{z} + v\tilde{z})dx - \tilde{\lambda}\int_{\Gamma_N} v\tilde{z}dx \\
&= \int_\Omega \nabla v \cdot K(\mu)\nabla\tilde{z}dx - \tilde{\lambda}\int_\Omega (\nabla v \cdot \nabla\tilde{z} + v\tilde{z})dx - \tilde{\lambda}\int_{\Gamma_N} v\tilde{z}dx \\
&\quad - \tilde{\lambda}\int_\Omega (\nabla v \cdot q + v\nabla \cdot q)dx + \tilde{\lambda}\int_{\Gamma_N} vq \cdot nds \\
&= \tilde{\lambda}\int_\Omega v(-\tilde{z} - \nabla \cdot q)dx + \tilde{\lambda}\int_\Omega \nabla v \cdot (\tilde{\lambda}^{-1}K(\mu)\nabla\tilde{z} - \nabla\tilde{z} - q)dx - \tilde{\lambda}\int_{\Gamma_N} v(\tilde{z} - q \cdot n)ds \\
&\le (\|v\|^2_{L^2(\Omega)} + \|\nabla v\|^2_{L^2(\Omega)} + \|v\|^2_{L^2(\Gamma_N)})^{1/2} \\
&\quad \tilde{\lambda}(\|\nabla \cdot q + \tilde{z}\|^2_{L^2(\Omega)} + \|q - \tilde{\lambda}^{-1}K(\mu)\nabla\tilde{z} + \nabla\tilde{z}\|^2_{L^2(\Omega)} + \|q \cdot n - \tilde{z}\|^2_{L^2(\Gamma_N)})^{1/2} \\
&= \|v\|_{\mathcal{W}}(F_{\text{eig}}(\tilde{z}, \tilde{\lambda}, q; \mu))^{1/2};
\end{aligned}$$

here, the second equality follows from the Green's theorem. It thus follows

$$\|r_{\text{eig}}(\cdot; \tilde{z}, \tilde{\lambda}; \mu)\|_{\mathcal{W}'} \equiv \sup_{v \in \mathcal{V}} \frac{r_{\text{eig}}(\cdot; \tilde{z}, \tilde{\lambda}; \mu)}{\|v\|_{\mathcal{W}}} \le (F_{\text{eig}}(\tilde{z}, \tilde{\lambda}, q; \mu))^{1/2},$$

which is the desired inequality. ∎

4.6. Finite element approximation of $\tau_{\text{LB}}(\mu)$. We now present a practical algorithm to compute $\tau_{\text{LB}}(\mu)$ for select values of μ in the offline stage. As before, we use conforming finite-element approximation spaces $\mathcal{V}^{\mathcal{N}_\mathcal{V}} \subset \mathcal{V}$ and $\mathcal{Q}^{\mathcal{N}_\mathcal{Q}} \subset \mathcal{Q}$ defined in (13) and (14). We then seek the Galerkin finite element approximation of the eigenproblem (20): given $\mu \in \mathcal{D}$, find $(z_1^{\mathcal{N}}(\mu), \lambda_1^{\mathcal{N}}(\mu)) \in \mathcal{V}^{\mathcal{N}_\mathcal{V}} \times \mathbb{R}$ such that

$$a(z_1^{\mathcal{N}}(\mu), v; \mu) = \lambda_1^{\mathcal{N}}(\mu)(z_1^{\mathcal{N}}(\mu), v)_{\mathcal{W}} \quad \forall v \in \mathcal{V}^{\mathcal{N}_\mathcal{V}}. \tag{28}$$

We then compute a minimum-residual approximation $\zeta^{\mathcal{N}}(\mu) \in \mathcal{Q}^{\mathcal{N}_\mathcal{Q}}$ which minimizes the dual norm bound:

$$\zeta^{\mathcal{N}}(\mu) = \arg\inf_{q \in \mathcal{Q}^{\mathcal{N}_\mathcal{Q}}} F_{\text{eig}}(z_1^{\mathcal{N}}(\mu), \lambda_1^{\mathcal{N}}(\mu), q; \mu) \tag{29}$$

Finally, *assuming* $|\lambda_1^{\mathcal{N}}(\mu) - \lambda_1(\mu)| < |\lambda_1^{\mathcal{N}}(\mu) - \lambda_2(\mu)|$, we appeal to Corollary 9 and Proposition 10 to construct a lower bound of $\tau(\mu)$,

$$\tau_{\text{LB}}^{\mathcal{N}}(\mu) \equiv \lambda_1^{\mathcal{N}}(\mu) - (F_{\text{eig}}(z_1^{\mathcal{N}}(\mu), \lambda_1^{\mathcal{N}}(\mu), \zeta^{\mathcal{N}}(\mu); \mu))^{1/2} \le \lambda_1(\mu). \tag{30}$$

We emphasize that the superscript $\mathcal{N}$ on $\tau_{\text{LB}}^{\mathcal{N}}(\mu)$ signifies that the lower bound approximation is computed in the $\mathcal{O}(\mathcal{N})$-dimensional finite element space, and it does *not* signify that the lower bound is with respect to the finite element eigenproblem; the lower bound is indeed with respect to the infinite-dimensional eigenproblem (20).

4.7. Exact-space SCM: offline-online computation of $\tau_{\mathrm{LB},M}(\mu)$. We can summarize the exact-space SCM as follows. In the offline stage, we prepare the space

$$\tilde{\mathcal{Y}}_{\mathrm{LB}}(\Xi_{\mathrm{con}}) \equiv \left\{ y \in \tilde{B}_{Q_K} \mid \sum_{q=1}^{Q_K} \Theta_q^K(\mu') y_q \geq \tau_{\mathrm{LB}}^{\mathcal{N}}(\mu'),\ \forall \mu' \in \Xi_{\mathrm{con}} \right\},$$

where $\tau_{\mathrm{LB}}^{\mathcal{N}}(\mu')$, $\mu' \in \Xi_{\mathrm{con}}$, are computed by (30) and $\tilde{B}_{Q_K} \equiv \prod_{q=1}^{Q_K} [\tilde{\gamma}_q^-, \tilde{\gamma}_q^+]$, where $\tilde{\gamma}_q^{\pm}$, $q = 1, \ldots, Q_K$, are computed by (24) and (25).

In the online stage, we solve the linear programming problem

$$\tau_{\mathrm{LB},M}(\mu) \equiv \inf_{y \in \tilde{\mathcal{Y}}_{\mathrm{LB}}(\Xi_{\mathrm{con}})} \mathcal{J}(\mu; y),$$

which provide a lower bound of $\tau(\mu)$. We then compute a lower bound of the stability constant $\alpha(\mu; \delta)$,

$$\alpha_{\mathrm{LB},M}(\mu; \delta) \equiv 1 + \frac{\delta}{\tau_{\mathrm{LB},M}(\mu)} \leq \alpha(\mu; \delta). \tag{31}$$

The subscript M on $\tau_{\mathrm{LB},M}(\mu)$ and $\alpha_{\mathrm{LB},M}(\mu; \delta)$ signifies the cardinality of the constraint set: $M \equiv |\Xi_{\mathrm{con}}|$.

4.8. Galerkin reduced basis method: offline-online computation of $\tau_{\mathrm{UB},M}(\mu)$. While the lower bound of $\tau(\mu)$ is needed to construct error bounds, an upper bound of $\tau(\mu)$ is useful to assess the sharpness of our lower bound, especially in the context of adaptive mesh refinement and parameter sampling. The evaluation of an upper bound is significantly simpler than the evaluation of a lower bound; we may simply appeal to Galerkin projection onto a subspace.

At the finite element level, $\lambda_1^{\mathcal{N}}(\mu)$ associated with the eigenproblem (28) is an upper bound of the exact first eigenvalue $\lambda(\mu)$. The upper bound property follows from $\lambda_1(\mu) = \inf_{v \in \mathcal{V}} |||v|||_\mu / \|v\|_{\mathcal{W}} \leq \inf_{v \in \mathcal{V}^{\mathcal{N}}} |||v|||_\mu / \|v\|_{\mathcal{W}} = \lambda_1^{\mathcal{N}}(\mu)$ for $\mathcal{V}^{\mathcal{N}} \subset \mathcal{V}$. We hence set $\tau_{\mathrm{UB}}^{\mathcal{N}}(\mu) = \lambda_1^{\mathcal{N}}(\mu)$. We then readily compute the (relative) bound gap $|\tau_{\mathrm{UB}}^{\mathcal{N}}(\mu) - \tau_{\mathrm{LB}}^{\mathcal{N}}(\mu)| / \tau_{\mathrm{UB}}^{\mathcal{N}}(\mu)$, which serves as an error estimate.

At the reduced basis level, we first construct a reduced basis space

$$\mathcal{V}_M^{\mathrm{eig}} = \mathrm{span}\{ z_1^{\mathcal{N}}(\mu') \}_{\mu' \in \Xi_{\mathrm{con}}};$$

here in principle the snapshot parameters need not be the same as the SCM constraint set Ξ_{con}; however, in practice, we use the same set of parameters because the finite element snapshots $(z_1^{\mathcal{N}}(\mu'), \lambda_1^{\mathcal{N}}(\mu'))$, $\mu' \in \Xi_{\mathrm{con}}$, are generated as a biproduct of evaluating $\tau_{\mathrm{LB}}^{\mathcal{N}}(\mu')$, $\mu' \in \Xi_{\mathrm{con}}$, as described in Section 4.6. We then solve a reduced basis eigenproblem: given $\mu \in \mathcal{D}$, find $(z_{M,1}(\mu), \lambda_{M,1}(\mu)) \in \mathcal{V}_M^{\mathrm{eig}} \times \mathbb{R}$ such that

$$a(z_{M,1}(\mu), v; \mu) = \lambda_{M,1}(\mu)(z_{M,1}(\mu), v)_{\mathcal{W}} \quad \forall v \in \mathcal{V}_M^{\mathrm{eig}};$$

the Galerkin approximation is an upper bound of the exact first eigenvalue: we hence set $\tau_{\mathrm{UB},M}(\mu) \equiv \lambda_{M,1}(\mu) \geq \lambda_1(\mu)$. We note that this reduced basis eigenproblem admits offline-online computational decomposition. Hence, the combination of $\tau_{\mathrm{UB},M}(\mu)$ from the reduced basis eigenproblem and $\tau_{\mathrm{LB},M}(\mu)$ from the SCM allows us to rapidly evaluate for any $\mu \in \mathcal{D}$ the (relative) bound gap $|\tau_{\mathrm{UB},M}(\mu) - \tau_{\mathrm{LB},M}(\mu)| / \tau_{\mathrm{UB},M}(\mu)$, which serves as an error estimate.

5. Error bounds.

5.1. Energy norm. Given our reduced basis approximation (16) to the PDE (1), our computable, online-efficient bound is given by,

$$|||u(\mu) - u_N(\mu)|||_\mu \leq \Delta_N^{\mathrm{en}}(\mu) \equiv \frac{1}{(\alpha_{\mathrm{LB},M}(\mu; \delta))^{1/2}} (F(u_N(\mu), p_N(\mu); \mu; \delta))^{1/2}, \tag{32}$$

where $F(\cdot, \cdot; \cdot; \cdot)$ is the bound form (8), and $\alpha_{\mathrm{LB},M}(\cdot; \cdot)$ is the lower bound of the stability constant associated with the SCM approximation (31).

5.2. Linear functional output. As discussed in Section 2.4, the energy-norm error bound may be readily extended to provide an error bound for linear functional outputs. We here sketch the procedure. We first introduce an adjoint residual bound form: for any $\mu \in \mathcal{D}$, $\delta \in \mathbb{R}_{>0}$, $\tilde{\psi} \in \mathcal{V}$, and $q \in \mathcal{Q}$,

$$F_{\text{adj}}(\tilde{\psi}, q; \mu; \delta) \equiv \|\nabla\tilde{\psi} - K^{-1}(\mu)q\|^2_{\mathcal{K}(\mu)} + \delta^{-1}\|f^o(\mu) + \nabla \cdot q\|^2_{L^2(\Omega)} + \delta^{-1}\|g^o(\mu) - q \cdot n\|^2_{L^2(\Gamma_N)},$$

where f^o and g^o define the output functional $\ell^o(\cdot;\mu)$ as given by (5). Following the same steps as Proposition 5 for the (primal) residual, we can readily show that the adjoint residual bound form satisfies $\|r_{\text{adj}}(\cdot;\tilde{\psi};\mu)\|_{\mathcal{V}'(\mu;\delta)} \le (F_{\text{adj}}(\tilde{\psi}, q; \mu; \delta))^{1/2}$, $\forall q \in \mathcal{Q}$. We then introduce the minimum-bound mixed finite element approximation of the adjoint problem (6): given $\mu \in \mathcal{D}$ and $\delta \in \mathbb{R}_{>0}$, find $\{\psi^{\mathcal{N}}(\mu), q^{\mathcal{N}}(\mu)\} \in \mathcal{V}^{\mathcal{N}_\mathcal{V}} \times \mathcal{Q}^{\mathcal{N}_\mathcal{Q}}$ such that

$$\{\psi^{\mathcal{N}}(\mu), q^{\mathcal{N}}(\mu)\} = \underset{\substack{v \in \mathcal{V}^{\mathcal{N}_\mathcal{V}} \\ q \in \mathcal{Q}^{\mathcal{N}_\mathcal{Q}}}}{\arg\inf} F_{\text{adj}}(v, q; \mu; \delta).$$

Similarly, given reduced-basis approximation spaces for the adjoint, $\mathcal{V}_N^{\text{adj}} \subset \mathcal{V}^{\mathcal{N}_\mathcal{V}}$ and $\mathcal{Q}_N^{\text{adj}} \subset \mathcal{Q}^{\mathcal{N}_\mathcal{Q}}$, we introduce the minimum-bound mixed reduced basis approximation of the adjoint problem (6): given $\mu \in \mathcal{D}$ and $\delta \in \mathbb{R}_{>0}$, find $\{\psi_N(\mu), q_N(\mu)\} \in \mathcal{V}_N^{\text{adj}} \times \mathcal{Q}_N^{\text{adj}}$ such that

$$\{\psi_N(\mu), q_N(\mu)\} = \underset{\substack{v \in \mathcal{V}_N^{\text{adj}} \\ q \in \mathcal{Q}_N^{\text{adj}}}}{\arg\inf} F_{\text{adj}}(v, q; \mu; \delta).$$

Following Proposition 4, we define the adjoint-corrected reduced basis approximation of the output as

$$s_N(\mu) \equiv \ell^o(u_N(\mu);\mu) + r(\psi_N(\mu); u_N(\mu); \mu),$$

and endow the estimate with a computable, online-efficient output bound

$$|s(\mu) - s_N(\mu)| \le \Delta_N^s(\mu) \equiv \frac{1}{\alpha_{\text{LB},M}(\mu;\delta)}(F(u_N(\mu), p_N(\mu); \mu; \delta))^{1/2}(F_{\text{adj}}(\psi_N(\mu), q_N(\mu); \mu; \delta))^{1/2}. \tag{33}$$

We again emphasize that this output bound is with respect to the exact output and not the finite element "truth" approximation.

One particular output that is relevant in engineering analysis of coercive systems is the *compliance output* $s(\mu) = \ell(u(\mu);\mu)$, which is associated with the internal energy in the system. Note that for compliance output, $\ell^o(\cdot;\cdot) = \ell(\cdot;\cdot)$, the primal problem (1) and the adjoint problem (6) are identical, and the solutions satisfy $\psi(\mu) = u(\mu)$. In addition, we have $F(\cdot,\cdot;\cdot;\cdot) = F_{\text{adj}}(\cdot,\cdot;\cdot;\cdot)$, $\psi^{\mathcal{N}}(\mu) = u^{\mathcal{N}}(\mu)$, and, for $\mathcal{V}_N = \mathcal{V}_N^{\text{adj}}$ and $\mathcal{Q}_N = \mathcal{Q}_N^{\text{adj}}$, $\psi_N(\mu) = u_N(\mu)$. Consequently, for the compliance output, we have $s_N(\mu) = \ell(u_N(\mu);\mu) + r(u_N(\mu); u_N(\mu); \mu)$ and $\Delta_N^s(\mu) = F(u_N(\mu), p_N(\mu); \mu; \delta)/\alpha_{\text{LB},M}(\mu;\delta) = (\Delta_N^{\text{en}}(\mu))^2$. The compliance output is not only engineering relevant, but also simplifies certain computational aspects while exercising the most important aspects of exact error bounds and spatio-parameter adaptive algorithms that will be discussed in Section 6. We will hence consider this compliance output in the numerical example in Section 7.

6. Spatio-parameter adaptivity.

6.1. Adaptive finite element for the stability eigenproblem. Although we employ the finite element approximation simply as a means to evaluate $\tau_{\text{LB}}^{\mathcal{N}}(\mu')$, $\mu' \in \Xi_{\text{con}}$, required in the online stage, we nevertheless wish to compute $\tau_{\text{LB}}^{\mathcal{N}}(\mu')$ efficiently and minimize the computational effort to achieve a given accuracy. Towards this end, we solve the eigenproblem using an adaptive finite element method.

We drive our adaptive finite element method using the standard solve, estimate, mark, and refine strategy (see, e.g., [21]). Towards this end, we must define an error indicator for each element $\kappa \in \mathcal{T}_h$. We use the following elemental residual indicator for our finite element approximation of the eigenpair $(z_1^{\mathcal{N}}(\mu), \lambda_1^{\mathcal{N}}(\mu)) \in \mathcal{V}^{\mathcal{N}_\mathcal{V}} \times \mathbb{R}$ given by (28) and the associated dual field $\zeta^{\mathcal{N}}(\mu) \in \mathcal{Q}^{\mathcal{N}_\mathcal{Q}}$ given by (29):

$$\begin{aligned}\eta_{\text{eig},\kappa} \equiv (\lambda_1^{\mathcal{N}}(\mu))^2(&\|\nabla \cdot \zeta^{\mathcal{N}}(\mu) + z_1^{\mathcal{N}}(\mu)\|^2_{L^2(\kappa)} + \|\zeta^{\mathcal{N}}(\mu) - (\lambda_1^{\mathcal{N}}(\mu))^{-1}K(\mu)\nabla z_1^{\mathcal{N}}(\mu) + \nabla z_1^{\mathcal{N}}(\mu)\|^2_{L^2(\kappa)} \\ &+ \|\zeta^{\mathcal{N}}(\mu) \cdot n - z_1^{\mathcal{N}}(\mu)\|^2_{L^2(\partial\kappa \cap \Gamma_N)}), \quad \kappa \in \mathcal{T}_h.\end{aligned}$$

Algorithm 1: Spatio-parameter adaptive SCM

input : $\Xi_{\text{train}} \subset \mathcal{D}$: SCM training set
ϵ_{SCM}: greedy bound-gap tolerance
$\epsilon_{\text{SCM,FE}}$: adaptive finite element tolerance
$M_{\max}$: maximum permissible number of finite element solves

output: $\{\tau_{\text{LB}}^{\mathcal{N}}(\mu')\}_{\mu' \in \Xi_{\text{con}}}$: SCM constraints
$\mathcal{V}_M^{\text{eig}} = \{z_1^{\mathcal{N}}(\mu')\}_{\mu' \in \Xi_{\text{con}}}$: RB eigenproblem space

Set $\mu^{(1)}$ to the approximate centroid: $\mu^{(1)} = \arg\min_{\mu \in \Xi_{\text{train}}} \|\mu - \bar{\mu}\|_{\ell^2}$ for $\bar{\mu} = \frac{1}{|\Xi_{\text{train}}|} \sum_{\mu \in \Xi_{\text{train}}} \mu$.

for $M = 2, \ldots, M_{\max}$ **do**

Identify the parameter associated with the largest relative $\tau(\mu)$ gap

$$\mu^{(M)} = \arg\sup_{\mu \in \Xi_{\text{train}}} (\tau_{\text{UB},M-1}(\mu) - \tau_{\text{LB},M-1}(\mu))/\tau_{\text{UB},M-1}(\mu);$$

if $\sup_{\mu \in \Xi_{\text{train}}} (\tau_{\text{UB},M}(\mu) - \tau_{\text{LB},M}(\mu))/\tau_{\text{UB},M}(\mu) < \epsilon_{\text{SCM}}$, terminate.

Solve (28) and (30) to obtain an upper bound $\tau_{\text{UB}}^{\mathcal{N}}(\mu^{(M)})$ and a lower bound $\tau_{1,\text{LB}}^{\mathcal{N}}(\mu)$; invoke mesh adaptivity as necessary such that $(\tau_{\text{UB}}^{\mathcal{N}}(\mu_M) - \tau_{\text{LB}}^{\mathcal{N}}(\mu_M))/\tau_{\text{UB}}^{\mathcal{N}}(\mu) < \epsilon_{\text{SCM,FE}}$

Augment the SCM constraint set,

$$\Xi_{\text{con}} \leftarrow \Xi_{\text{con}} \cup \mu^{(M)},$$

and update $\{\tau_{\text{LB}}^{\mathcal{N}}(\mu')\}_{\mu' \in \Xi_{\text{con}}}$ and $\mathcal{V}_M^{\text{eig}} = \{z_1^{\mathcal{N}}(\mu')\}_{\mu' \in \Xi_{\text{con}}}$ accordingly.

end

Note that $\eta_{\text{eig},\kappa}$ is an elemental contribution to the eigenvalue bound gap in the sense that

$$\sum_{\kappa \in \mathcal{T}_h} \eta_{\text{eig},\kappa} = F_{\text{eig}}(z_1^{\mathcal{N}}(\mu), \lambda_1^{\mathcal{N}}(\mu), y^{\mathcal{N}}(\mu); \mu) = \tau_{\text{UB}}^{\mathcal{N}}(\mu) - \tau_{\text{LB}}^{\mathcal{N}}(\mu).$$

Once we identify elements with biggest contributions to the eigenvalue bound gap, we employ a fixed-fraction marking strategy to mark top 5% of the elements for refinement. We repeat the solve-estimate-mark-refine process until the desired bound-gap tolerance is met.

6.2. Spatio-parameter adaptive SCM. We select the SCM constraint points Ξ_{con} and evaluate the associated constraints $\{\tau_{\text{LB}}^{\mathcal{N}}(\mu')\}_{\mu' \in \Xi_{\text{con}}}$ using the adaptive algorithm described in Algorithm 1. As in the original SCM [7], we construct the constraint set $\Xi_{\text{con}} \subset \Xi_{\text{train}}$ by selecting the constraint parameters in a greedy manner based on the bound gap; however, we emphasize that, unlike the original SCM, this bound gap is associated with the stability constant with respect to the infinite-dimesional space $\mathcal{V}$. Once we identify the next constraint point, we then solve the eigenproblem using the adaptive finite element method described in Section (6.1). The finite element approximation that meets the tolerance requirement is then included in the updated reduced basis set $\mathcal{V}_N^{\text{eig}}$. The greedy procedure continues until the relative bound gap is smaller than the specified tolerance at all training points.

We make a few remarks regarding the choice of the inputs. First, as in the original SCM [7], we select a sufficiently rich training set Ξ_{train} to cover the parameter domain $\mathcal{D}$. Second, again similar to the original SCM [7], we in theory require $\epsilon_{\text{SCM}} \in (0, 1)$ but in practice select $\epsilon_{\text{SCM}} \in [0.5, 0.9]$. However, unlike in the original SCM, a loose bound gap tolerance ϵ_{SCM} does not directly affect the effectivity of the stability constant $\alpha_{\text{LB},M}(\mu; \delta)$; this is due to the transformation of the stability constant described in Section 4.1, which desensitizes the effectivity of $\alpha_{\text{LB},M}(\mu; \delta)$ from the effectivity of $\tau_{\text{LB},M}(\mu)$ for δ sufficiently small. Third, in theory, we require that $\epsilon_{\text{SCM,FE}} \leq \epsilon_{\text{SCM}}$; in practice, we select $\epsilon_{\text{SCM,FE}} \approx \epsilon_{\text{SCM}}/10$. This selection criteria is similar to that used for the reduced basis counterpart in the spatio-parameter Greedy algorithm that is described shortly, and whose choice is analyzed in detail in Appendix B. A tighter tolerance in general increases the lower bound provided at the constraint points and decreases the number of constraint points

M to achieve a given ϵ_{SCM}. The online cost will hence decrease for a smaller $\epsilon_{\text{SCM,FE}}/\epsilon_{\text{SCM}}$. The offline cost on the other hand may decrease or increase: a smaller $\epsilon_{\text{SCM,FE}}/\epsilon_{\text{SCM}}$ reduces the number of eigenproblems to be solved, but increases the cost associated with the approximation of each eigenproblem.

6.3. Selection of δ. While the residual bound introduced in Proposition 5 and the $\alpha(\mu;\delta)$-$\tau(\mu)$ relationship described in Proposition 7 hold for any $\delta \in \mathbb{R}_{>0}$, we in practice select δ sufficiently small such that the effectivity of $\alpha_{\text{LB},M}(\mu;\delta)$ is desensitized from the effectivity of $\tau_{\text{LB},M}(\mu)$, which can be quite poor for the SCM. In practice, we set

$$\delta = \frac{1}{10} \inf_{\mu \in \Xi_{\text{train}}} \tau_{\text{LB},M}(\mu).$$

This choice ensures that

$$\inf_{\mu \in \Xi_{\text{train}}} \alpha_{\text{LB},M}(\mu;\delta) = \inf_{\mu \in \Xi_{\text{train}}} \left(1 + \frac{\delta}{\tau_{\text{LB},M}(\mu)}\right)^{-1} \geq \frac{10}{11}.$$

The stability constant $\alpha_{\text{LB},M}(\mu;\delta)$ is guaranteed to be close to unity for all $\mu \in \Xi_{\text{train}}$; in practice, $\alpha_{\text{LB},M}(\mu;\delta)$ is close to unity for all $\mu \in \mathcal{D}$ given $\Xi_{\text{train}} \subset \mathcal{D}$ is sufficiently rich.

6.4. Adaptive finite element for the solution. Similar to the approximation of the stability eigenproblem considered in Section 6.1, we also employ an adaptive finite element method based on the solve-estimate-mark-refine strategy to approximate the solution $u(\mu)$ (see, e.g., [21]). A residual indicator associated with an element $\kappa \in \mathcal{T}_h$ for our finite element approximation $u^{\mathcal{N}}(\mu) \in \mathcal{V}^{\mathcal{N}_\mathcal{V}}$ and $p^{\mathcal{N}}(\mu) \in \mathcal{Q}^{\mathcal{N}_\mathcal{Q}}$ is

$$\begin{aligned}\eta_\kappa \equiv \|\nabla u^{\mathcal{N}}(\mu) - K^{-1}(\mu) p^{\mathcal{N}}(\mu)\|^2_{\mathcal{K}(\mu),\kappa} + \delta^{-1}\|f(\mu) + \nabla \cdot p^{\mathcal{N}}(\mu)\|^2_{L^2(\kappa)} \\ + \delta^{-1}\|g(\mu) - p^{\mathcal{N}}(\mu)\cdot n\|^2_{L^2(\partial\kappa \cap \Gamma_N)}, \quad \kappa \in \mathcal{T}_h.\end{aligned}$$

Note that η_κ is an element contribution to the residual in the sense that

$$\sum_{\kappa \in \mathcal{T}_h} \eta_\kappa = F(u^{\mathcal{N}}(\mu), p^{\mathcal{N}}(\mu); \mu; \delta).$$

As in the adaptive procedure for the stability eigenproblem, we use a fixed-fraction marking strategy with a threshold of 5% for our adaptive mesh refinement.

6.5. Spatio-parameter adaptive weak Greedy algorithm. Our spatio-parameter adaptive weak Greedy algorithm was originally introduced in [23] to control the dual norm of the residual with respect to the exact space $\mathcal{V}$; here we apply the algorithm to control the energy-norm or functional-output error. Specifically, the goal of the weak greedy algorithm is to drive the quantity $\Delta_N(\mu)/\omega_N(\mu)$ to be less than a user specified threshold $\epsilon_{\text{RB}} > 0$ in an automated manner [18]. Here, the error bound $\Delta_N(\mu)$ can be the energy-norm bound $\Delta^{\text{en}}_N(\mu)$ defined in (32) or the output bound $\Delta^{\text{s}}_N(\mu)$ defined in (33); $\omega_N(\mu)$ is a normalization function, which would be 1 if the goal is to control the absolute energy or output error. In the numerical example in Section 7, we will control the relative compliance output error, for which $\Delta_N(\mu) \equiv \Delta^{\text{s}}_N(\mu) = (\Delta^{\text{en}}_N(\mu))^2$ and $\omega_N(\mu) \equiv s_N(\mu)$.

We select the reduced basis sampling points using the adaptive algorithm described in Algorithm 2. As in the standard weak Greedy algorithm [18], we choose the sampling point $\mu^{(N)}$ in a greedy manner based on the error bound $\Delta_N(\mu)$; however, unlike in the standard Greedy algorithm, this error bound is associated with the exact solution $u(\mu) \in \mathcal{V}$ as opposed to the finite element "truth" solution. Once we identify the next sampling parameter, we find the associated solution using the adaptive finite element method described in Section 6.4. We then augment our reduced basis spaces $\mathcal{V}_N$ and $\mathcal{Q}_N$ with the new snapshot. The greedy procedure is repeated until the quantity $\Delta_N(\mu)/\omega_N(\mu)$ is smaller than the specified threshold at all training points.

We make a few remarks regarding the choice of the inputs. First, as in the standard weak Greedy algorithm [18], we select a sufficiently rich training set Ξ_{train} to cover the parameter domain $\mathcal{D}$; in practice

Algorithm 2: Spatio-parameter adaptive weak Greedy algorithm

input : Ξ_{train}: reduced basis training set
ϵ_{RB}: greedy error tolerance
$\epsilon_{\text{RB,FE}}$: adaptive finite element tolerance
$N_{\max}$: maximum permissible number of finite element solves
output: $\mathcal{V}_N$, $\mathcal{Q}_N$: reduced basis spaces

for $N = 1, \ldots, N_{\max}$ **do**
  Identify the parameter associated with the largest error bound

$$\mu^{(N)} = \arg\sup_{\mu \in \Xi_{\text{train}}} \frac{\Delta_{N-1}(\mu)}{\omega_{N-1}(\mu)};$$

  if $\sup_{\mu \in \Xi_{\text{train}}} \Delta_{N-1}(\mu)/\omega_{N-1}(\mu) \leq \epsilon_{\text{RB}}$, terminate.
  Solve (15) to obtain finite element approximations $u^{\mathcal{N}}(\mu^{(N)})$ and $p^{\mathcal{N}}(\mu^{(N)})$; invoke mesh adaptivity as necessary such that $\Delta^{\mathcal{N}}(\mu)/\omega^{\mathcal{N}}(\mu) \leq \epsilon_{\text{RB,FE}}$.
  Augment the reduced basis spaces

$$\mathcal{V}_N = \text{span}\{\mathcal{V}_{N-1}, u^{\mathcal{N}}(\mu^{(N)})\} \quad \text{and} \quad \mathcal{Q}_N = \text{span}\{\mathcal{Q}_{N-1}, p^{\mathcal{N}}(\mu^{(N)})\}.$$

end

we use the same training set as that used for the SCM. Second, in theory, we require that $\epsilon_{\text{RB,FE}} \leq \epsilon_{\text{RB}}$; this is a sufficient condition to ensure that $\max_{\mu \in \Xi_{\text{train}}} \Delta_N(\mu)/\omega_N(\mu) \leq \epsilon_{\text{RB}}$ for some N sufficiently large because *i*) each snapshot will satisfy the target tolerance ϵ_{RB} and *ii*) the error bound associated with the minimum-bound formulation is a non-increasing function of the dimension of the reduced basis space N for any given μ. Third, in practice, we set $\epsilon_{\text{RB,FE}} \approx \epsilon_{\text{RB}}/10$; this choice is required to ensure that the convergence of the spatio-parameter greedy algorithm does not slow down as the maximum error level approaches the target ϵ_{RB}. A more detailed discussion on the choice of $\epsilon_{\text{RB,FE}}$ is provided in Appendix B. Finally, we note that ϵ_{RB}, and not $\epsilon_{\text{RB,FE}}$, ultimately controls the accuracy of the reduced basis model.

6.6. Mesh refinement mechanics: working and common spaces. Our spatio-parameter adaptive algorithms require the computation of the inner product of two finite element fields associated with two different spaces. In order to compute various inner products, we employ two different types of meshes: a "working mesh" which is used to compute the current finite element solution $u^{\mathcal{N}}(\mu)$ and $p^{\mathcal{N}}(\mu)$ or the current finite element eigenfunction $z_1^{\mathcal{N}}(\mu)$ and $\zeta^{\mathcal{N}}(\mu)$; a "common mesh" which is a superset of all working meshes used in the greedy algorithm. Whenever we need to compute the inner product of two fields associated with two different spaces, we re-represent the fields on the common space and then perform the inner product algebraically.

REMARK 11. *In our current implementation, we keep a single common mesh and perform inner product between any two finite element fields on the common mesh. Alternatively, we could compute a common mesh that is a superset of just two fields whose inner product we wish to evaluate. This latter approach could reduce the computational cost, especially if the finite element mesh required for various parameter values differ considerably; on the other hand, the approach would require multiple solutions of the mesh intersection problem.*

6.7. Remarks on the spatio-parameter adaptive algorithm. We make four remarks about the reduced basis model constructed by our spatio-parameter adaptive algorithm. First, for any parameter $\mu \in \mathcal{D}$, regardless of whether it belongs to Ξ_{train}, our reduced model provides a (normalized) error bound $\Delta_N(\mu)/\omega_N(\mu)$ with respect to the exact solution $u(\mu) \in \mathcal{V}$, and not the typical finite element "truth" solution, in complexity independent of the size of the finite element spaces.

Second, if the parameter μ belongs to the training set Ξ_{train}, then the (normalized) error bound

$\Delta_N(\mu)/\omega_N(\mu)$ is guaranteed to be less than the training tolerance: $\Delta_N(\mu)/\omega_N(\mu) \leq \epsilon_{\text{RB}}$, $\forall \mu \in \Xi_{\text{train}}$. In other words, we certify the reduced basis approximation for any $\mu \in \mathcal{D}$, and the certificate is less than ϵ_{RB} for $\mu \in \Xi_{\text{train}}$.

Third, the proposed algorithm is fundamentally different from the following two-step approach: *i*) we invoke the standard reduced-basis Greedy algorithm with an error bound with respect to the finite element "truth" to identify the worst case; *ii*) we compute the reduced basis snapshot using an adaptive finite element method. In the online stage, this two step approach would only provide an error bound with respect to the finite element "truth" for a general $\mu \in \mathcal{D}$, and an error bound with respect to the exact solution for snapshot parameters. Hence, the two-step approach would not certify the reduced basis approximation with respect to the exact solution for an arbitrary $\mu \in \mathcal{D}$.

Fourth, both spatio-parameter adaptive SCM and weak Greedy algorithms can be extended in various ways. For instance, the adaptive finite element solvers could employ *hp* and/or anisotropic adaptation (e.g., [20]) to further reduce the cost associated with the computation of the snapshots. Similarly, the parameter sampling algorithms could use *hp* partitioning in the parameter space (e.g., [5]); the *hp* partitioning may be necessary particularly for high dimensional problems.

7. Numerical example: thermal block.

7.1. Problem description. We demonstrate the proposed reduced basis method for the thermal block problem [18]. The problem is defined on a unit square domain, $\Omega \equiv [0,1]^2$, shown in Figure 1(a), and a $P = 9$-dimensional parameter domain $\mathcal{D} = [10^{-1/2}, 10^{1/2}]^9 \subset \mathbb{R}^9$. The weak statement for the problem is the following: given $\mu \in \mathcal{D}$, find $u(\mu) \in \mathcal{V} \equiv \{v \in H^1(\Omega) \mid v|_{\Gamma_{\text{top}}} = 0\}$ such that

$$\sum_{i=1}^{P} \int_{\Omega_i} \nabla v \cdot \mu_i \nabla w dx = \int_{\Gamma_{\text{bottom}}} v ds \quad \forall v \in \mathcal{V},$$

and then evaluate the compliance output

$$s(\mu) = \int_{\Gamma_{\text{bottom}}} u(\mu) ds.$$

Note that we impose homogeneous Dirichlet boundary condition on Γ_{top}, homogeneous Neumann boundary condition on Γ_{side}, and inhomogeneous Neumann condition on Γ_{bottom}. The equation satisfies all assumptions described in Section 2.1: it is coercive for all $\mu \in \mathcal{D}$, the diffusivity field admits affine decomposition, the inverse of the diffusivity admits affine decomposition, and all fields are piecewise polynomial. Specifically, our affine decompositions are given by $K(\mu) = \sum_{q=1}^{P} \Theta_q^K(\mu) K_q = \sum_{q=1}^{Q_K \equiv P} \mu_q \mathbb{1}_{\Omega_q}$ and $K^{-1}(\mu) = \sum_{q=1}^{Q_{K^{\text{inv}}} \equiv P} \Theta_q^{K^{\text{inv}}}(\mu) K_q^{\text{inv}} = \sum_{q=1}^{P} \frac{1}{\mu_q} \mathbb{1}_{\Omega_q}$, where $\mathbb{1}_{\Omega_q}$ is the indicator function associated with a subdomain $\Omega_q \subset \Omega$.

We consider this thermal block problem because, while it is simple, it exhibits parameter-dependent spatial singularities. For instance, when all the diffusion coefficients are equal to 1.0, the solution is given by $u(x_1, x_2) = 1 - x_2$, exhibiting no spatial singularities. On the other hand, when the diffusivity coefficients associated with four subdomains that share a corner are different, then the solution becomes singular at the corner. See, e.g., Figure 5 for such singular solutions.

7.2. Limitations of the standard reduced basis method. Before applying the proposed spatio-parameter adaptive method to the thermal block problem, we solve the problem using the standard reduced basis method to highlight its limitations. Towards this end, we employ the Galerkin reduced basis method, whose snapshots are computed in a fixed "truth" $\mathbb{P}^2$ finite element space using the weak Greedy method. (See, e.g., [18] for details.)

Figure 1(b) shows the convergence of the standard reduced basis method for the problem using two uniform "truth" spaces with $\mathcal{N} = 625$ and $\mathcal{N} = 9409$. The figure shows the "truth" error bound — with respect to the finite element "truth" output — and the approximate actual error — with respect to the reference output s_{ref} computed accurately to a relative toleance of 0.001 — as a function of the dimension of the reduced basis space. First, focusing on the actual error, we observe that the convergence of the standard reduced basis method stagnates at the error level of ≈ 0.04 and ≈ 0.013 for the two "truth" spaces of the

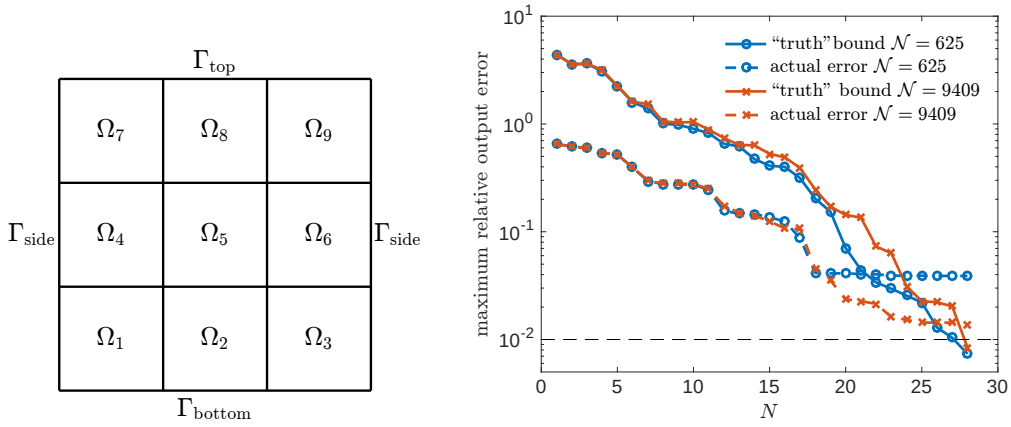

(a) Geometry

(b) convergence of standard RB method

FIG. 1. *Thermal block problem. (a) Geometry. (b) The maximum relative "truth" error bound,* $\max_{\mu\in\Xi_{\text{train}}} \Delta_N^{\text{s,std}}(\mu)/s_N^{\text{std}}(\mu)$*, and the maximum actual relative error,* $\max_{\mu\in\Xi_{\text{train}}} |s_{\text{ref}}(\mu) - s_N^{\text{std}}(\mu)|/|s_{\text{ref}}(\mu)|$*, for the standard reduced basis method. Here,* s_{ref} *denotes the reference output computed accurately to a relative tolerance of 0.001, and* s_N^{std} *and* $\Delta_N^{\text{s,std}}$ *denote the output and "truth" error bound, respectively, computed using a standard reduced basis method.*

size $\mathcal{N} = 625$ and $\mathcal{N} = 9409$, respectively; this behavior is anticipated due to the lack of spatial resolution at singularities. Second, focusing on the "truth" error bound, we observe that the "truth" does not serve as a bound with respect to the exact solution when substantial error due to the lack of spatial resolution is present. Of course, the use of a finer finite element truth space would mitigate these issues; however, in practice, a systematic identification of an appropriate "truth" space for problems that exhibit parameter-dependent singularities requires exhaustive exploration of the parameter space using (say) an adaptive finite element method, and in any event the prediction provided by the reduced model is never rigorously certified with respect to the exact solution. These behaviors of the standard reduced basis method motivate the use of the proposed method with an exact solution certificate and spatio-parameter adaptivity.

7.3. Spatio-parameter greedy training of the stability constant. We first note that, for the thermal block problem, we readily obtain

$$\gamma_q^- = \inf_{v\in\mathcal{V}} \frac{\int_\Omega \nabla v \cdot K_q \nabla v dx}{\|v\|_{\mathcal{W}}^2} = \inf_{v\in\mathcal{V}} \frac{\int_{\Omega_q} \nabla v \cdot \nabla v dx}{\|v\|_{\mathcal{W}}^2} \geq 0, \quad q = 1, \ldots, Q_K,$$
$$\gamma_q^+ = \sup_{v\in\mathcal{V}} \frac{\int_\Omega \nabla v \cdot K_q \nabla v dx}{\|v\|_{\mathcal{W}}^2} \leq \|\lambda_{\max}(K_q)\|_{L^\infty(\Omega)} = \|\mathbb{1}_{\Omega_q}\|_{L^\infty(\Omega)} = 1, \quad q = 1, \ldots, Q_K.$$

To select the SCM constraint set Ξ_{con}, we invoke the spatio-parameter adaptive SCM algorithm, Algorithm 1, with the following inputs. We choose a training set Ξ_{train} that contains $2^9 = 512$ corner points of the nine-dimesional parameter domain $\mathcal{D}$, 2000 random points in $\mathcal{D}$, and the midpoint of $\mathcal{D}$; the total size of the training set is 2513. We choose the SCM and finite element relative bound gap tolerance of $\epsilon_{\text{SCM}} = 0.8$ and $\epsilon_{\text{SCM,FE}} = 0.002$, respectively. We choose a 6×6 $\mathbb{P}^2$ finite element space as the initial approximation space. We note that this initial mesh is somewhat finer than the initial mesh that will be used for the reduced basis training; this initial refinement is intended to ensure that $\lambda_1^{\mathcal{N}}(\mu)$ even on the initial mesh is closer to $\lambda_1(\mu)$ than to $\lambda_2(\mu)$, though again we have no means to verify if the condition is met.

The result of the training is summarized in Figure 2. Figure 2(a) shows the convergence of the bound gap with the cardinality of the SCM constraint set M. We require $M = 10$ SCM constraints to meet the relative bound gap threshold of $\epsilon_{\text{SCM}} = 0.8$; the bound gap decreases slowly initially, but for $M = 10$ the relative bound gap is $\approx 0.68 < \epsilon_{\text{SCM}}$. Figure 2(b) shows the distribution of the lower and upper bound of $\tau(\mu)$ for the 2513 training points. For this particular problem, we could determine through inspection that $\tau(\mu)$ is bounded from below by 10^{-1}; indeed, the minimum $\tau(\mu)$ over the training set computed with the

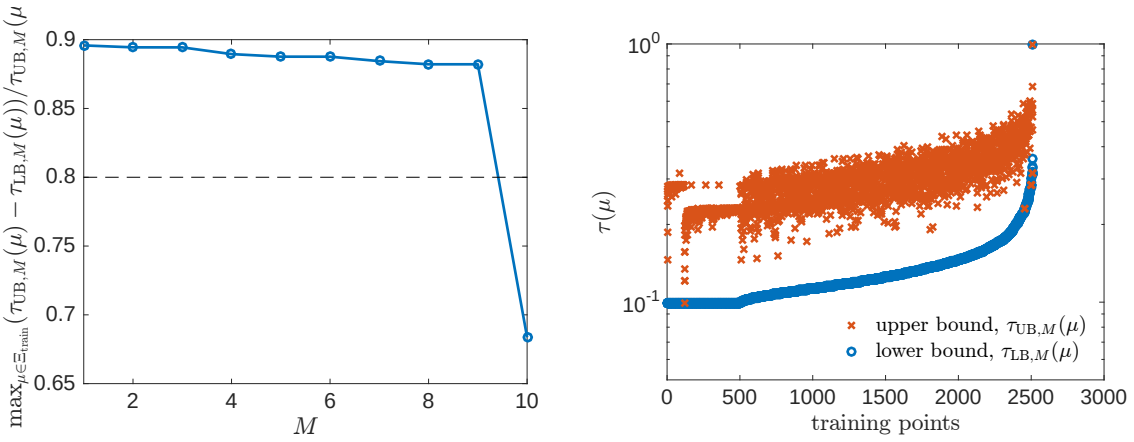

(a) relative bound gap

(b) final bounds

FIG. 2. *Spatio-parameter greedy SCM training for* $\tau_{\mathrm{LB},M}(\mu)$ *and* $\tau_{\mathrm{UB},M}(\mu)$.

SCM algorithm is also ≈ 0.1. We will hence set $\delta = 0.09$ in our minimum-residual reduced basis method.

Figure 3 summarizes the behavior of the adaptive finite element method for the stability eigenproblem for two of the cases. The first case, shown in Figures 3(a), 3(d), and 3(c), is associated with the second SCM constraint $\mu^{(2)}$, which is the most difficult case in terms of $\mathcal{N}$ required to meet the bound gap tolerance at $\mathcal{N} = 1066$. The diffusivity is $10^{-1/2}$ for bottom middle block (Ω_2) and is $10^{1/2}$ for the remaining blocks. Figure 3(a) shows the first eigenfunction. Figure 3(d) shows the associated final adapted mesh. We observe that the adaptive finite element targets the bottom middle boundary as well as the two singularities at two of the corners of Ω_2; we also note that the smallest element has the edge length of $2^{-8}/3$, implying that a uniform refinement that achieves the same resolution at the singularity would require over 2×10^6 as opposed to $\mathcal{N} = 1066$ for the adaptive method. Figure 3(c) shows the evolution of the upper and lower bound of the first eigenvalue, $\tau^{\mathcal{N}}_{\mathrm{UB}}(\mu^{(2)})$ and $\tau^{\mathcal{N}}_{\mathrm{LB}}(\mu^{(2)})$, with finite element adaptation; we meet the desired relative bound gap of $\epsilon_{\mathrm{SCM,FE}} = 0.002$ after 11 adaptation iterations.

The second case, shown in Figures 3(b), 3(e), and 3(c), is associated with the fifth SCM constraint $\mu^{(5)}$, which is one of the easier cases in terms of $\mathcal{N}$ required to meet the bound gap tolerance at $\mathcal{N} = 236$. The diffusivity is $10^{-1/2}$ for the middle block (Ω_2) and is $10^{1/2}$ for the remaining blocks. Figure 3(b) shows the first eigenfunction. Figure 3(e) shows the associated final adapted mesh; we observe that only the middle block is refined, and the refinement is not as aggressive as that observed for $\mu^{(2)}$ in Figure 3(d). Figure 3(c) shows the evolution of the upper and lower bound of the first eigenvalue; we need only three adaptation iterations to meet the target relative bound gap tolerance.

Figure 3(f) shows the final common mesh for $M = 10$. The common space is of size $\mathcal{N} = 2568$ and is refined towards singularities that are present for *some of* the training parameters. As a result, the common mesh is larger than any of the working meshes, whose size vary from $\mathcal{N} = 216$ to $\mathcal{N} = 1066$; however, we recall that the common mesh is simply used to compute various inner products between snapshots and never used to solve the eigenproblem. It is also worth noting that the smallest element has the edge length of $2^{-8}/3$, which implies that a uniform mesh with the same resolution at the singularity would require over 2×10^6 degrees of freedom.

7.4. Spatio-parameter greedy training of reduced basis. We now train our reduced basis using the spatio-parameter adaptive Greedy algorithm, Algorithm 2, with the following inputs. We choose a training set Ξ_{train} that is identical to that used for the SCM training described in Section 7.3. We choose the target relative output error tolerance of $\epsilon_{\mathrm{RB}} = 0.01$. We choose the finite element relative output error tolerance of $\epsilon_{\mathrm{RB,FE}} = 0.002$. We choose a 3×3 $\mathbb{P}^2$ finite element space as the initial approximation space. The weight parameter, as discussed in Section 7.3, is $\delta = 0.09 < (1/10) \arg\inf_{\mu \in \Xi_{\mathrm{train}}} \tau_{\mathrm{LB},M}(\mu)$.

Figure 4 summarizes the behavior of the spatio-parameter Greedy algorithm. The total of $N = 26$

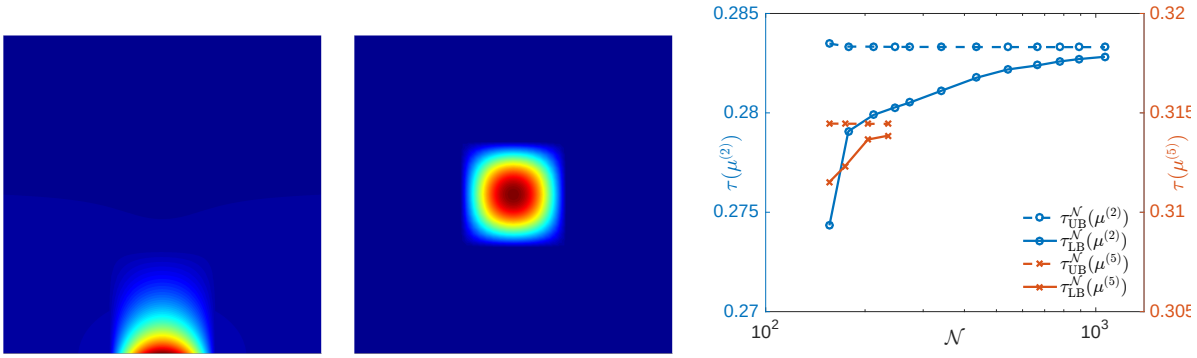

(a) eigenfunction, $\mu^{(2)}$ (b) eigenfunction, $\mu^{(5)}$ (c) bound, $\mu^{(2)}$

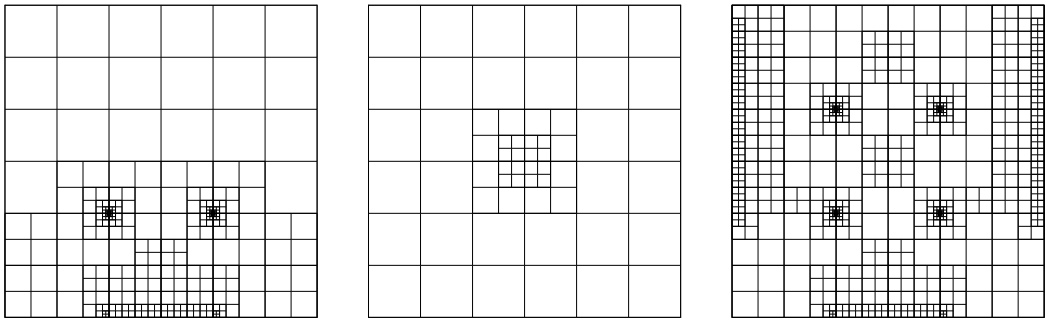

(d) mesh, $\mu^{(2)}$ (e) mesh, $\mu^{(5)}$ (f) final common mesh

FIG. 3. *Adaptive finite element approximation of the stability eigenproblem. The parameter values are* $\mu^{(2)} = (10^{1/2}, 10^{-1/2}, 10^{1/2}, 10^{1/2}, 10^{1/2}, 10^{1/2}, 10^{1/2}, 10^{1/2}, 10^{1/2})$ *and* $\mu^{(5)} = (10^{1/2}, 10^{1/2}, 10^{1/2}, 10^{1/2}, 10^{-1/2}, 10^{1/2}, 10^{1/2}, 10^{1/2}, 10^{1/2})$.

reduced basis functions are required to meet the relative error tolerance of 0.01. Figure 4(a) shows the variation in the size of the working mesh used to approximate the solution for the 26 parameter values; the size of the of problem varies from $\mathcal{N} = 126$ for the first parameter to $\mathcal{N} = 4868$ for the ninth parameter. We note that each of these spaces is significantly smaller than the finer "truth" space considered for the standard reduced basis method in Section 7.2, which nevertheless is inadequate to deliver the required accuracy. Figure 4(b) shows the convergence of the relative error bound with the size of the reduced basis space N; we observe that the error bound decreases exponentially with N. In addition, we observe that the error bound is an effective estimate of the actual error with respect to the reference solution computed accurately to a relative tolerance of 0.001.

Figure 5 summarizes the behavior of the adaptive finite element method for two cases. The first case, shown in Figures 5(a), 5(d), and 5(c), is associated with the fourth reduced basis function $\mu^{(4)}$, which is one of the easiest cases requiring only $\mathcal{N} = 230$ to meet the error tolerance. Figure 5(a) shows the solution. Figure 5(d) shows the associated final adapted mesh; the mesh is largely unchanged from the initial coarse mesh aside from some refinement in the bottom right region. Figure 5(c) shows the error convergence; we need only two adaptation iterations to meet the error tolerance. We also observe that the effectivity of the error bound is ≈ 2, which is quite tight; here, for comparison purposes, the reference solution is computed using the adaptive finite element with an error tolerance 100 times smaller than the target finite element error tolerance of $\epsilon_{\mathrm{RB,FE}} = 0.002$.

The second case, shown in Figures 5(b), 5(e), and 5(c), is associated with the fourth reduced basis function $\mu^{(9)}$, which is the most difficult case in terms of $\mathcal{N}$ required to meet the error tolerance at $\mathcal{N} = 4868$. Figure 5(b) shows the solution; note that the top six blocks form a checkerboard pattern, resulting in two strong singularities. Figure 5(e) shows the associated final adapted mesh. The mesh is strongly graded

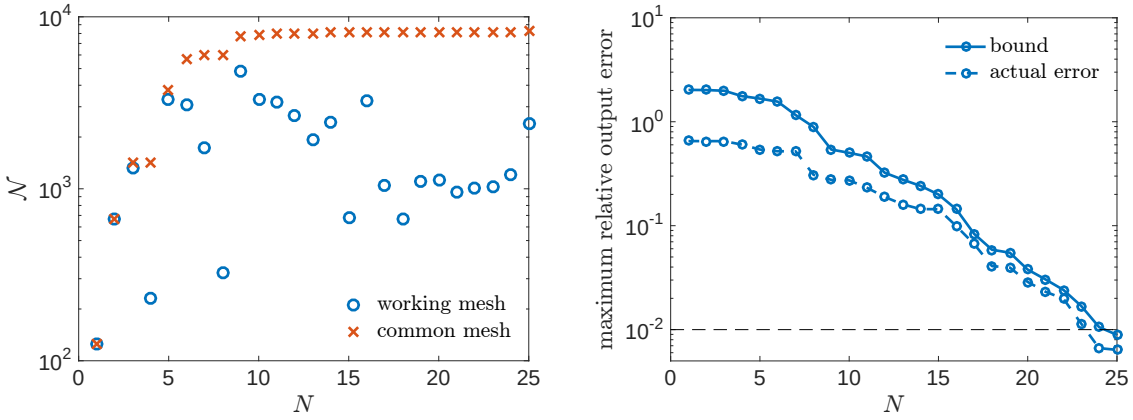

(a) degrees of freedom (b) error bound

FIG. 4. *Spatio-parameter greedy reduced-basis training. In (b), the maximum relative output error bound is given by* $\max_{\mu\in\Xi_{\text{train}}} \Delta_N^s(\mu)/s_N(\mu)$ *and the maximum relative output error is given by* $\max_{\mu\in\Xi_{\text{train}}} |s_{\text{ref}}(\mu) - s_N(\mu)|/|s_{\text{ref}}(\mu)|$. *Here,* s_{ref} *denotes the reference output computed accurately to a relative tolerance of* 10^{-3}.

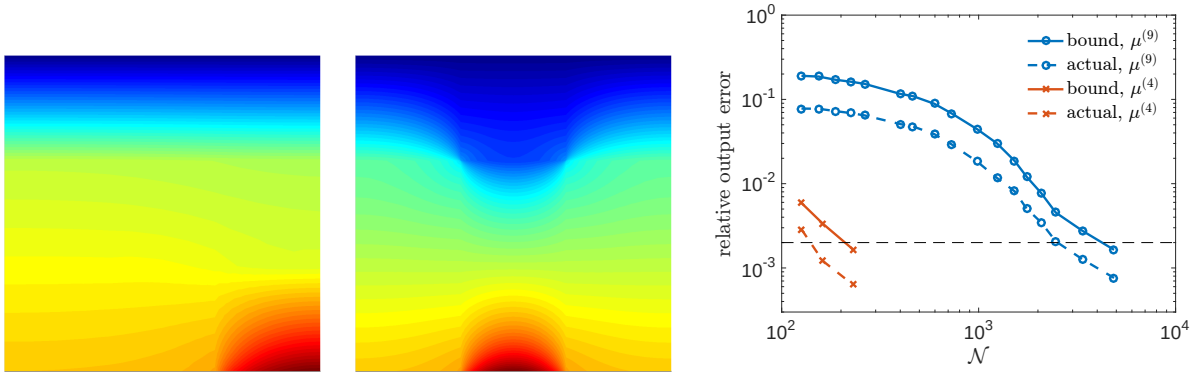

(a) solution, $\mu^{(4)}$ (b) solution, $\mu^{(9)}$ (c) error convergence

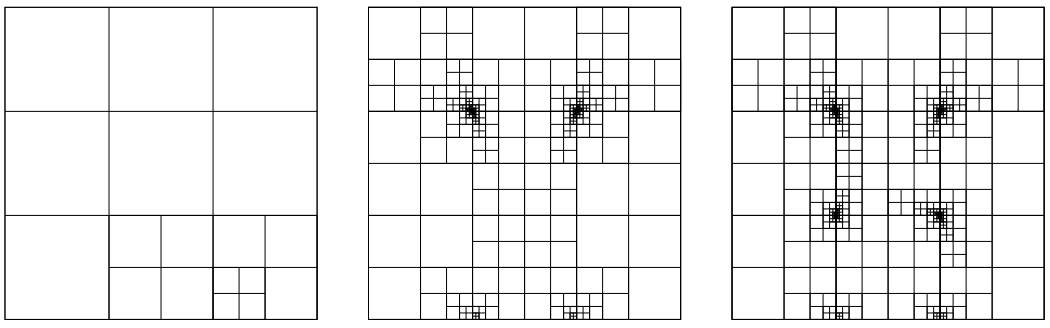

(d) mesh, $\mu^{(4)}$ (e) mesh, $\mu^{(9)}$ (f) final common mesh

FIG. 5. *Adaptive finite element approximation of the solution. In (c), for* $\mu^{(i)}$, $i = 4, 9$, *the relative output error bound is given by* $\Delta^{s,\mathcal{N}}(\mu^{(i)})/|s^{\mathcal{N}}(\mu^{(i)})|$ *and the actual relative output error is given by* $|s_{\text{ref}}(\mu^{(i)}) - s^{\mathcal{N}}(\mu^{(i)})|/|s_{\text{ref}}(\mu^{(i)})|$. *Here,* s_{ref} *denotes the reference output, and* $s^{\mathcal{N}}$ *and* $\Delta^{s,\mathcal{N}}$ *denote the output and the error bound, respectively, associated with the finite element approximation. The parameter values are* $\mu^{(4)} = (10^{1/2}, 10^{1/2}, 10^{-1/2}, 10^{1/2}, 10^{1/2}, 10^{1/2}, 10^{-1/2}, 10^{-1/2}, 10^{-1/2})$ *and* $\mu^{(9)} = (10^{1/2}, 10^{-1/2}, 10^{1/2}, 10^{1/2}, 10^{-1/2}, 10^{1/2}, 10^{-1/2}, 10^{1/2}, 10^{-1/2})$.

towards two of the corners of Ω_5; the edge length of the smallest element is $2^{-10}/3$, which implies that a uniform mesh with the same resolution at the singularity would require $\approx 4 \times 10^7$ degrees of freedom as opposed to $\mathcal{N} = 4868$ for the adaptive mesh. Figure 5(c) shows the error convergence; we require 16 adaptation iterations to resolve the singularities and meet the error tolerance. The effectivity of the error bound is ≈ 3, which is again quite tight.

Figure 5(f) shows the final common mesh for $N = 26$. The common mesh is of size $\mathcal{N} = 8264$ and is aggressively refined towards singularities that are present for *some of* the training parameters; the edge length of the smallest element is $2^{-10}/3$, which implies that a uniform mesh with the same resolution at the singularity would require $\approx 4 \times 10^7$ degrees of freedom. We again emphasize that our spatio-parameter adaptive algorithm computes each snapshot on an adapted mesh specifically tailored for the parameter value; the common mesh is used only to evaluate various inner products of the snapshots. Hence, the cost associated with the computation of a snapshot of a given accuracy is reduced in our spatio-parameter adaptive reduced basis method relative to the standard reduced basis method that uses a fixed "truth" mesh.

Before concluding this section, we make one observation. While the second case analyzed associated with $\mu^{(9)}$ is a difficult case that exhibit a checkerboard pattern in the upper six blocks, none of the $N = 26$ snapshots is associated with the full nine-block checkerboard configuration for which strong singularities are present at all four corners of Ω_5. We note that this configuration is included in our training set Ξ_{train}. Hence, our reduced basis method provides an approximation that meets the tolerance of $\epsilon_{\text{RB}} = 0.01$ for this most difficult configuration even though a snapshot is never explicitly computed for the configuration. This is because some of the $N = 26$ snapshots provide basis functions that resolve the singularities at the lower corners of Ω_5, and hence a linear combination of all $N = 26$ snapshots effectively approximates the nine-block checkerboard solution.

8. Summary. We present a reduced basis method for parametrized coercive equations with two objectives: providing error bounds with respect to the exact weak solution in an infinite-dimensional space; providing reliable and efficient construction of a reduced basis model through adaptivity in both physical and parameter spaces. The proposed method builds on two key ingredients: a minimum-residual mixed formulation; an extension of the SCM to the infinite-dimesional function space. Both ingredients build on a duality-based approach and admits offline-online computational decomposition. We demonstrate the effectiveness of the proposed approach using the classical thermal block problem which exhibits parameter-dependent singularities; the spatio-parameter algorithm significantly reduces the offline computational cost, providing spatial resolution that would be computationally prohibitive with a uniform mesh. We also emphasize that the reduced model training using the spatio-parameter adaptive algorithm is fully automatic as the user need not worry about the choice of the snapshot parameters or the fidelity of the "truth" space. This automatic and reliable training is expected to play increasingly important role as the spatial and parametric complexity of problems we wish to solve continue to increase.

However, we note the error bound procedures as presented also have a number of limitations. First, the method is limited to linear coercive equations; as discussed in the introduction, to our knowledge, this is a limitation shared by essentially all computational techniques that provide uniform (as opposed to asymptotic) error bounds (as opposed to estimates). Second, even with the transformation for the stability constant which improves the effectivity of the SCM, the SCM can still require a large number of constraint points for complex cases; however, to our knowledge, the SCM is the only method that can provide uniform (as opposed to asymptotic) lower bound of the stability constant in an offline-online efficient manner. Due to these limitations, the construction of truly rigorous offline-online computable error bounds for more general problems is expected to pose significant challenges. In order to bring spatio-parameter adaptivity to more general classes of problems, it may be necessary to relax the requirement from uniform error bounds to, for instance, asymptotic error bounds or error estimates.

Acknowledgments. I would like to thank Prof. Anthony Patera of MIT for the many fruitful discussions and Prof. Bernard Haasdonk of University of Stuttgart for Remark 11 regarding the pair-wise common meshes. I would also like to thank the anonymous reviewers for the constructive feedback, which has helped improve the quality of this manuscript. This work was supported by OSD/AFOSR/MURI Grant FA9550-09-1-0613, ONR Grant N00014-11-1-0713, and the University of Toronto Institute for Aerospace Studies

(UTIAS) startup fund.

Appendix A. Error bounds without an affine decomposition of $K^{-1}(\mu)$. The error bound described in Sections 3 and 4 relies on the affine decomposition of $K^{-1}(\mu)$ given by (2). As noted in Remark 1, it is also possible to construct energy-norm and functional-output error bounds — with respect to the exact weak solution — without this assumption. In this appendix, we sketch the construction of this alternative bound and outline tradeoffs with respect to the proposed bound.

The alternative bound is obtained by computing the dual norm of the residual and the stability constant with respect to the (non-parametrized) norm (18), given by $\|\cdot\|_{\mathcal{W}} \equiv \|\cdot\|_{H^1(\Omega)} + \|\cdot\|_{L^2(\Gamma_N)}$, instead of the parametrized norm $\|\cdot\|_{\mathcal{V}(\mu;\delta)}$. For any $\mu \in \mathcal{D}$ and $\tilde{u} \in \mathcal{V}$, the dual norm of the residual is given by

$$\|r(\cdot;\tilde{u};\mu)\|_{\mathcal{W}} \equiv \sup_{v\in\mathcal{V}} \frac{r(v;\tilde{u};\mu)}{\|v\|_{\mathcal{W}}};$$

a bound form for this dual norm with respect to $\|\cdot\|_{\mathcal{W}}$ was introduced in our previous work [23]. The stability constant, which we denote by $\alpha_{\mathcal{W}}(\mu)$, is given by

$$\alpha_{\mathcal{W}}(\mu) \equiv \inf_{v\in\mathcal{V}} \frac{|||v|||_\mu^2}{\|v\|_{\mathcal{W}}^2};$$

we note that $\alpha_{\mathcal{W}}(\mu)$ is equal to the quantity $\tau(\mu)$ defined in (19), for which we have developed an exact-bound SCM in Section 4. Hence we may construct energy-norm and functional-output error bounds even in the absence of the affine decomposition of $K^{-1}(\mu)$.

One obvious advantage of this alternative formulation, relative to the formulation developed in Sections 3 and 4, is that the formulation works even when a convenient affine decomposition of $K^{-1}(\mu)$ does not exist. However it has two disadvantages. The first is the computational scaling of the quadratic term of the residual bound form, $G(\cdot,\cdot;\mu;\delta)$, with the number of terms in the affine expansion, Q_K; specifically, the number of terms for the alternative formulation is $\mathcal{O}(Q_K^2)$ instead of $\mathcal{O}(Q_K)$ for the original formulation. The second is the sharpness of the stability constant. Specifically, the effectivity of the stability constant for the alternative formulation, $\alpha_{\mathcal{W}}(\mu) = \tau(\mu)$, is the same as the effectivity of $\tau_{\text{LB}}(\mu)$; we do not benefit from the desensitization provided by the the transformation from $\alpha(\mu;\delta)$ to $\tau(\mu)$ as given in Proposition 7. The latter is particularly problematic, as a lower bound provided by the SCM, while rigorous, is often not very effective. For these reasons, we recommend the formulation described in Sections 3 and 4 for problems for which a convenient affine decomposition of $K^{-1}(\mu)$ exists.

Appendix B. The selection of $\epsilon_{\text{RB,FE}}$. In this appendix, we study the effect of the adaptive finite element tolerance, $\epsilon_{\text{RB,FE}}$, on the convergence of the spatio-parameter adaptive weak Greedy algorithm, Algorithm 2. We first note the minimum requirement for $\epsilon_{\text{RB,FE}}$ from a theoretical perspective. We observe that $\epsilon_{\text{RB,FE}} \le \epsilon_{\text{RB}}$ is required to ensure that the reduced basis approximations at the snapshot parameter values meet the required tolerance ϵ_{RB}. In fact, in principle, $\epsilon_{\text{RB,FE}} \le \epsilon_{\text{RB}}$ is the only required condition to obtain $\Delta_N^s(\mu)/s_N(\mu) \le \epsilon_{\text{RB}}$ for all $\mu \in \Xi_{\text{train}}$. This is because if each snapshot is computed accurately to the tolerance of ϵ_{RB}, we may in principle compute the snapshot at every $\mu \in \Xi_{\text{train}}$; thanks to the minimum-bound formulation which provides non-increasing sequence of bounds for any given parameter, this construction is guaranteed to yield a reduced basis model that meets the specified tolerance of ϵ_{RB} for all $\mu \in \Xi_{\text{train}}$. However, in practice we wish to use much fewer than $|\Xi_{\text{train}}|$ snapshots.

We now perform a numerical study to analyze the effect of $\epsilon_{\text{RB,FE}}$ using the thermal block problem considered in Section 7. Figure 6 shows the convergence of the spatio-parameter adaptive algorithm for a few different choices of $\epsilon_{\text{RB,FE}}$; here $\epsilon_{\text{RB,FE}}$ is expressed as a fraction of ϵ_{RB}. We observe that the number of snapshots, N, required to achieve a given error tolerance decreases for a smaller $\epsilon_{\text{RB,FE}}$. In fact, for $\epsilon_{\text{RB,FE}} = \epsilon_{\text{RB}}$, the convergence noticeably slows down as the maximum error approaches ϵ_{RB}. The two tighter choices of the finite element tolerance, $\epsilon_{\text{RB,FE}} = \epsilon_{\text{RB,FE}}/5$ and $\epsilon_{\text{RB,FE}} = \epsilon_{\text{RB,FE}}/20$, do not suffer from this slow convergence at the end. We speculate that the reduced basis systems constructed for these two values of $\epsilon_{\text{RB,FE}}$ are essentially the same as that obtained in the limit of $\epsilon_{\text{RB,FE}} \to 0$ with exact snapshots.

An appropriate choice of $\epsilon_{\text{RB,FE}}$ relative to ϵ_{RB} is dependent on the problem and also on the desired balance of the offline and online costs. In particular, the online cost decreases for a smaller $\epsilon_{\text{RB,FE}}/\epsilon_{\text{RB}}$ thanks

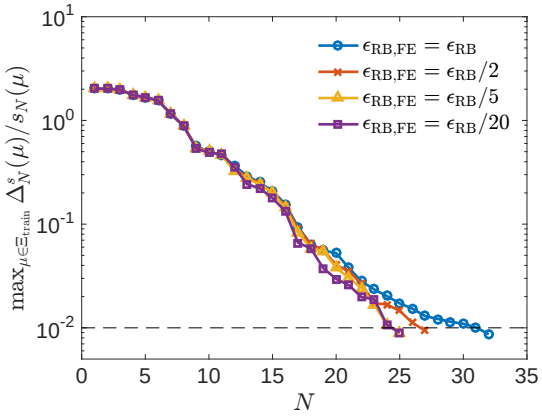

FIG. 6. *The convergence of the spatio-parameter adaptive algorithm for different choices of* $\epsilon_{\rm RB,FE}$.

to the reduced size of the reduced model. On the other hand, the offline cost may decrease or increase: a smaller $\epsilon_{\rm RB,FE}/\epsilon_{\rm RB}$ reduces the number of snapshots to be computed but increases the cost of computing each snapshot. Our recommendation is to use a value of $\epsilon_{\rm RB,FE}/\epsilon_{\rm FE} \approx 5$ to 20, which appears to work well for the problems we have considered to date.

REFERENCES

[1] M. AINSWORTH AND J. T. ODEN, *A posteriori error estimation in finite element analysis*, Comput. Methods Appl. Mech. Engrg., 142 (1997), pp. 1–88.

[2] M. ALI, K. STEIH, AND K. URBAN, *Reduced basis methods based upon adaptive snapshot computations*, (2015), p. submitted.

[3] P. B. BOCHEV AND M. D. GUNZBURGER, *Finite element methods of least-squares type*, SIAM Rev., 40 (1998), pp. 789–837.

[4] F. CHATELIN, *Spectral approximations of linear operators*, Academic Press, New York, 1983.

[5] J. L. EFTANG, A. T. PATERA, AND E. M. RØNQUIST, *An "hp" certified reduced basis method for parametrized elliptic partial differential equations*, SIAM J. Sci. Comput., 32 (2010), pp. 3170–3200.

[6] M. B. GILES AND E. SÜLI, *Adjoint methods for PDEs: a posteriori error analysis and postprocessing by duality*, in Acta Numerica, vol. 11, 2002, pp. 145–236.

[7] D. B. P. HUYNH, G. ROZZA, S. SEN, AND A. T. PATERA, *A successive constraint linear optimization method for lower bounds of parametric coercivity and inf-sup stability constants*, C. R. Acad. Sci. Paris, Ser. I, 345 (2007), pp. 473–478.

[8] T. KATO, *On the upper and lower bounds of eigenvalues*, J. Phys. Soc. Japan, 4 (1949), pp. 334–339.

[9] P. LADEVÈZE, *Strict upper error bounds on computed outputs of interest in computational structural mechanics*, Comput Mech, 42 (2008), pp. 271–286.

[10] P. LADEVÈZE AND L. CHAMOIN, *On the verification of model reduction methods based on the proper generalized decomposition*, Comput. Methods Appl. Mech. Engrg., 200 (2011), pp. 2032–2047.

[11] P. LADEVÈZE AND D. LEGUILLION, *Error estimate procedure in the finite element method and applications*, SIAM J. Numer. Anal., 20 (1983), pp. 485–509.

[12] M. OHLBERGER AND F. SCHINDLER, *Error control for the localized reduced basis multi-scale method with adaptive on-line enrichment*, SIAM J. Sci. Comput., 37 (2015), pp. A2865–A2895.

[13] N. PARÉS, J. BONET, A. HUERTA, AND J. PERAIRE, *The computation of bounds for linear-functional outputs of weak solutions to the two-dimensional elasticity equations*, Comput. Methods Appl. Mech. Engrg., 195 (2006), pp. 430–443.

[14] A. I. PEHLIVANOV, G. F. CAREY, AND R. D. LAZAROV, *Least-squares mixed finite elements for second-order elliptic problems*, SIAM J. Numer. Anal., 31 (1994), pp. 1368–1377.

[15] M. PLUM, *Guaranteed numerical bounds for eigenvalues*, in Spectral theory and computational methods of Sturm-Liouville problems, D. Hinton and P. W. Schaefer, eds., Dekker, New York, 1997, pp. 313–332.

[16] A. QUARTERONI AND A. VALLI, *Numerical Approximation of Partial Differential Equations*, Springer, New York, 1997.

[17] P. A. RAVIART AND J. M. THOMAS, *A mixed finite element method for 2nd order elliptic problems*, in Lect. Notes in Math. 606, Springer-Verlag, 1977, pp. 292–315.

[18] G. ROZZA, D. B. P. HUYNH, AND A. T. PATERA, *Reduced basis approximation and a posteriori error estimation for affinely parametrized elliptic coercive partial differential equations — application to transport and continuum mechanics*, Archives of Computational Methods in Engineering, 15 (2008), pp. 229–275.

[19] A. M. SAUER-BUDGE, J. BONET, A. HUERTA, AND J. PERAIRE, *Computing bounds for linear functionals of exact weak solutions to Poisson's equation*, SIAM J. Numer. Anal., 42 (2004), pp. 1610–1630.

[20] C. Schwab, *p- and hp- Finite Element Methods*, Oxford Science Publications, Great Clarendon Street, Oxford, UK, 1998.
[21] R. Verfürth, *A posteriori error estimation and adaptive mesh-refinement techniques*, J. Comput. Appl. Math., 50 (1994), pp. 67–83.
[22] M. Yano, *A reduced basis method with exact-solution certificates for steady symmetric coercive equations*, Comput. Methods Appl. Mech. Engrg., 287 (2015), pp. 290–309.
[23] M. Yano, *A minimum-residual mixed reduced basis method: exact residual certification and simultaneous finite-element and reduced-basis refinement*, Math. Model. Numer. Anal., 50 (2016), pp. 163–185.
[24] M. Yano, *A reduced basis method with an exact solution certificate and spatio-parameter adaptivity: application to linear elasticity*, in Modeling, Simulation, and Applications: Special Volume MoRePaS 2015, A. Quarteroni, ed., Springer, accepted.